SOLAR SPECTRUM FORMATION

Robert J. Rutten

[Sterrekundig Instituut Utrecht & Institutt for Teoretisk Astrofysikk Oslo]

Texts: R.J. Rutten, *"Radiative Transfer in Stellar Atmospheres"* (RTSA), my website
D. Mihalas, *"Stellar Atmospheres"*, 1970, 1978
G.B. Rybicki and A.P. Lightman, *"Radiative Processes in Astrophysics"*, 1979, 2004
M. Stix, *"The Sun"*, 1989, 2002/2004

examples of local, nonlocal, converted photons: white light corona coronium lines EUV corona EUV bright/dark [Zanstra & Bowen PN lines]

radiative transfer basics: basic quantities constant S_ν plane-atmosphere RT Eddington-Barbier cartoons

LTE 1D solar radiation escape: Planck continuous opacity LTE continuum Boltzmann-Saha LTE line equations LTE line cartoons solar ultraviolet spectrum VALIIIC temperature solar spectrum formation Ca II H&K versus Halpha

NLTE 1D solar radiation escape: bb processes bb rates bb equilibria scattering solar radiation processes VAL3C continuum formation radiative cooling VAL3C radiation budget realistic line cartoon Na D1 Ca II 8542 versus Halpha

MHD-simulated essolar radiation escape: Ca II H in 1D Na D1 in 3D non-E hydrogen in 2D

summary: RTSA rap

WHITE LIGHT CORONA

Stix section 9.1.3

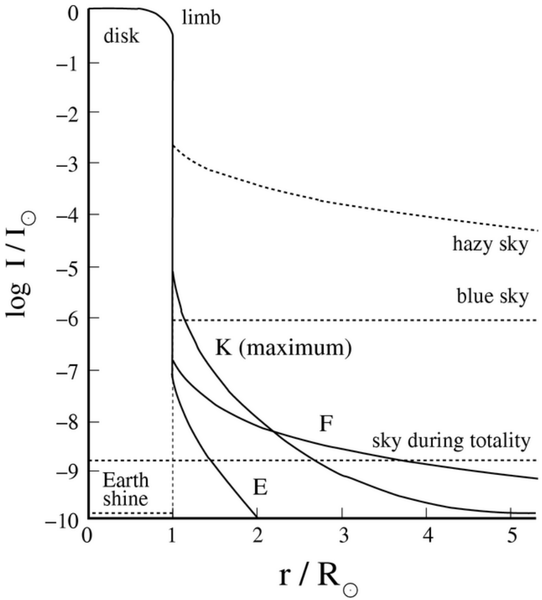

Grotrian (1931): Thomson scattering 8000 km s^{-1} electrons (S 9.2–9.3)

$$\rho^2 = x^2 + y^2 \qquad I(x) = 2\int_0^\infty j(\rho)\,\mathrm{d}y = 2\int_x^\infty \frac{\rho\ j(\rho)}{\sqrt{\rho^2 - x^2}}\,\mathrm{d}\rho$$

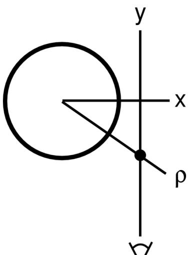

N_e from inverse Abel transform = isotropically scattered irradiation (S 9.4–9.5)

$$j(\rho) = -\frac{1}{\pi}\int_\rho^\infty \frac{\mathrm{d}I/\mathrm{d}x}{\sqrt{x^2-\rho^2}}\,\mathrm{d}x = \sigma_\mathrm{T}\,N_\mathrm{e}\,\frac{1}{4\pi}\int I_\odot(\theta)\,\mathrm{d}\Omega$$

"CORONIUM" LINES

Stix section 9.1.3 *http://laserstars.org/spectra/Coronium.html*

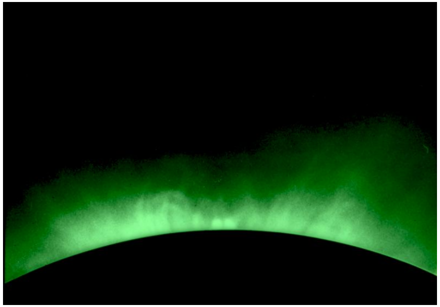

Grotrian, Edlén 1942: forbidden lines high ionization stages (Stix Table 9.2 p. 398)

name	wavelength	identification	$\Delta\lambda_D$	$\overline{v}$	A_{ul}	previous ion	$\chi_{\rm ion}$
green line	530.29 nm	[Fe XIV]	0.051 nm	29 km/s	60 s^{-1}	Fe XIII	355 eV
yellow line	569.45	[Ca XV]	0.087	46	95	Ca XIV	820
red line	637.45	[Fe XI]	0.049	23	69	Fe IX	235

Coronal sky at Dome C

EUV CORONA

Stix section 9.1.3

bf equilibria: collisional ionization = radiative recombination ⇒ only $f(T)$, not $f(N_e)$

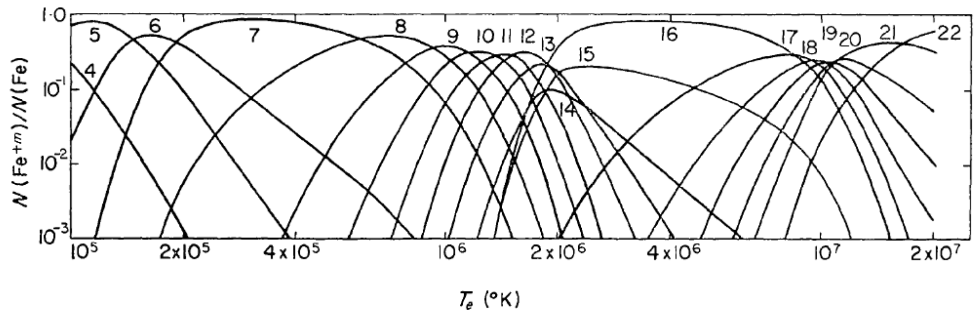

bb equilibria: collisional excitation = spontaneous deexcitation ⇒ $f(T, N_e)$ (S 9.9–9.10)

$$n_l C_{lu} = n_l N_e \int_{v_0}^{\infty} \sigma_{lu} f(v)\, v\, dv \approx n_u A_{ul} \qquad \sum h\nu \propto \int n_{ion} N_e \, dz = \int N_e^2 \left(\frac{dT}{dz}\right)^{-1} dT \equiv EM$$

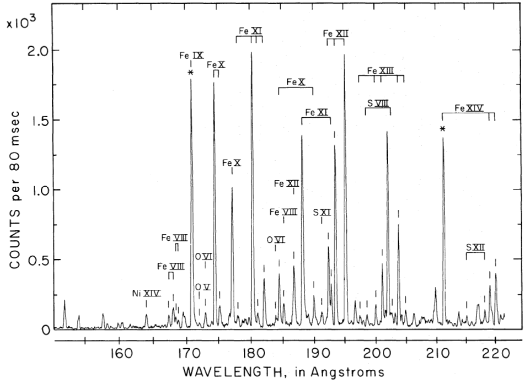

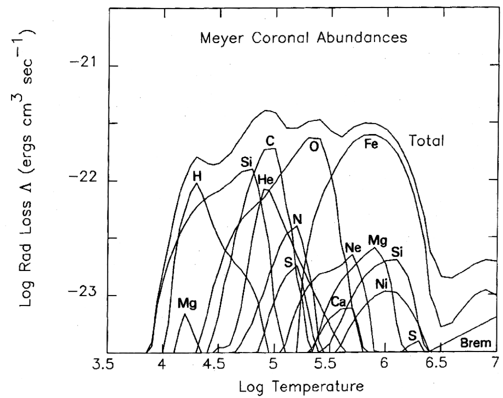

BRIGHT AND DARK IN EUV IMAGES

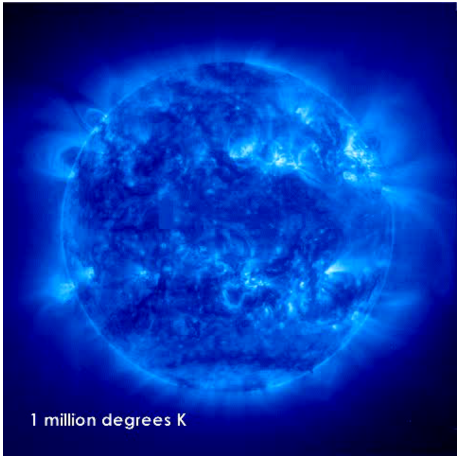

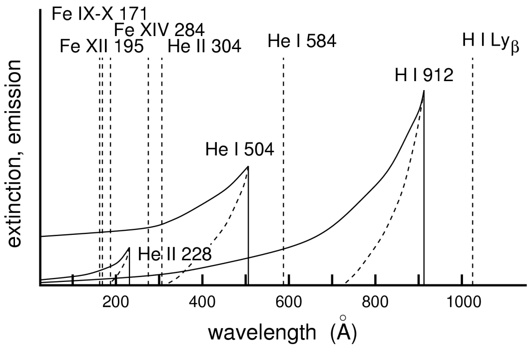

- *iron lines*
  - Fe IX/X 171 Å: about 1.0 MK
  - Fe XII 195 Å: about 1.5 MK
  - Fe XIV 284 Å: about 2 MK
- *bright*
  - collision up, radiation down
  - thermal photon creation, NLTE equilibrium
  - 171 Å: selected loops = special trees in forest
- *dark*
  - radiation up, re-radiation at bound-free edge
  - matter containing He^+, He, H: $10^4 - 10^5$ K
  - large opacity

BASIC QUANTITIES

RTSA 2.1–2.2, Stix 4.2.5

Monochromatic emissivity (Stix uses ε)

$$\mathrm{d}E_\nu \equiv j_\nu \,\mathrm{d}V \,\mathrm{d}t \,\mathrm{d}\nu \,\mathrm{d}\Omega \qquad \mathrm{d}I_\nu(s) = j_\nu(s)\,\mathrm{d}s$$

units j_ν: erg cm^{-3} s^{-1} Hz^{-1} ster^{-1} $\quad$ I_ν: erg cm^{-2} s^{-1} Hz^{-1} ster^{-1}

Monochromatic extinction coefficient

$$\mathrm{d}I_\nu \equiv -\sigma_\nu n\, I_\nu \,\mathrm{d}s \qquad \mathrm{d}I_\nu \equiv -\alpha_\nu\, I_\nu \,\mathrm{d}s \qquad \mathrm{d}I_\nu \equiv -\kappa_\nu \rho\, I_\nu \,\mathrm{d}s$$

units: cm^2 per particle (physics) $\quad$ cm^2 per cm^3 = per cm (RTSA) $\quad$ cm^2 per gram (astronomy)

Monochromatic source function

$$S_\nu \equiv j_\nu/\alpha_\nu = j_\nu/\kappa_\nu\rho \qquad S_\nu^{\mathrm{tot}} = \frac{\sum j_\nu}{\sum \alpha_\nu} \qquad S_\nu^{\mathrm{tot}} = \frac{j_\nu^c + j_\nu^l}{\alpha_\nu^c + \alpha_\nu^l} = \frac{S_\nu^c + \eta_\nu S_\nu^l}{1+\eta_\nu} \qquad \eta_\nu \equiv \alpha_\nu^l/\alpha_\nu^c$$

thick: (κ_ν, S_ν) more independent than (κ_ν, j_ν) $\quad$ stimulated emission negatively into α_ν, κ_ν

Transport equation with τ_ν as optical thickness along the beam

$$\frac{\mathrm{d}I_\nu}{\mathrm{d}s} = j_\nu - \alpha_\nu I_\nu \qquad \frac{\mathrm{d}I_\nu}{\alpha_\nu\,\mathrm{d}s} = S_\nu - I_\nu \qquad \mathrm{d}\tau_\nu \equiv \alpha_\nu\,\mathrm{d}s \qquad \frac{\mathrm{d}I_\nu}{\mathrm{d}\tau_\nu} = S_\nu - I_\nu$$

Plane-parallel transport equation with τ_ν as radial optical depth and μ as viewing angle

$$\mathrm{d}\tau_\nu \equiv -\alpha_\nu\,\mathrm{d}z \qquad \tau_\nu(z_0) = -\int_\infty^{z_0} \alpha_\nu\,\mathrm{d}z \qquad \mu \equiv \cos\theta \qquad \mu\,\frac{\mathrm{d}I_\nu}{\mathrm{d}\tau_\nu} = I_\nu - S_\nu$$

CONSTANT SOURCE FUNCTION

Transport equation along the beam (τ_ν = optical thickness)

$$\frac{\mathrm{d}I_\nu}{\mathrm{d}\tau_\nu} = S_\nu - I_\nu \qquad\qquad I_\nu(\tau_\nu) = I_\nu(0)\,\mathrm{e}^{-\tau_\nu} + \int_0^{\tau_\nu} S_\nu(t_\nu)\,\mathrm{e}^{-(\tau_\nu - t_\nu)}\,\mathrm{d}t_\nu$$

Invariant S_ν

$$I_\nu(D) = I_\nu(0)\,\mathrm{e}^{-\tau_\nu(D)} + S_\nu\left(1 - \mathrm{e}^{-\tau_\nu(D)}\right)$$

example: $S_\nu = B_\nu$ for all continuum and line processes in an isothermal cloud

Thick object

$$I_\nu(D) \approx S_\nu$$

Thin object

$$I_\nu(D) \approx I_\nu(0) + [S_\nu - I_\nu(0)]\;\tau_\nu(D) \qquad\qquad I_\nu(0) = 0:\;\; I_\nu(D) \approx \tau_\nu(D)\,S_\nu = j_\nu D$$

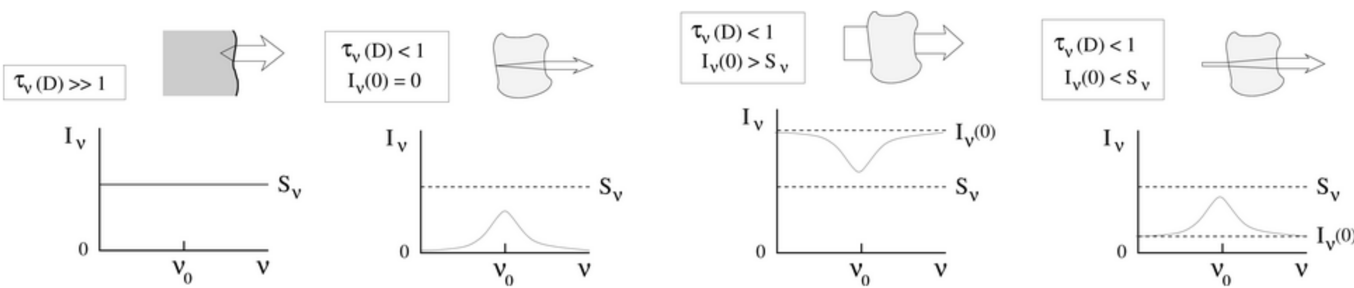

RADIATIVE TRANSFER IN A PLANE ATMOSPHERE

RTSA 2.2.2; Stix 4.1.1

Radial optical depth

$$\mathrm{d}\tau_\nu = -\kappa_\nu \rho \, \mathrm{d}r$$

r radial   Hubený $\tau_{\nu\mu}$ κ_ν cm^2/gram α_ν cm^{-1} = cm^2/cm^3 σ_ν cm^2/particle

Transport equation

$$\mu \frac{\mathrm{d}I_\nu}{\mathrm{d}\tau_\nu} = I_\nu - S_\nu$$

Integral form

$$I_\nu^-(\tau_\nu, \mu) = -\int_0^{\tau_\nu} S_\nu(t_\nu)\, \mathrm{e}^{-(t_\nu - \tau_\nu)/\mu} \, \mathrm{d}t_\nu/\mu \qquad I_\nu^+(\tau_\nu, \mu) = +\int_{\tau_\nu}^{\infty} S_\nu(t_\nu)\, \mathrm{e}^{-(t_\nu - \tau_\nu)/\mu} \, \mathrm{d}t_\nu/\mu$$

"formal solution"   NB: both directions   pm: Doppler anisotropy S_ν

Emergent intensity without irradiation

$$I_\nu(0, \mu) = (1/\mu) \int_0^\infty S_\nu(\tau_\nu)\ \mathrm{e}^{-\tau_\nu/\mu} \, \mathrm{d}\tau_\nu$$

Eddington-Barbier approximation

$$\boxed{I_\nu(0, \mu) \approx S_\nu(\tau_\nu = \mu)}$$

exact for linear $S_\nu(\tau_\nu)$

SIMPLE ABSORPTION LINE

- extinction: bb process gives peak in $\alpha_{\rm total} = \alpha_c + \alpha_l = (1+\eta_\nu)\,\alpha_c$
- optical depth: assume height-invariant $\alpha_{\rm total} \Rightarrow$ linear $(1+\eta_\nu)\,\tau_c$
- source function: assume same for line (bb) and continuous (bf, ff) processes
- use Eddington-Barbier (here nearly exact, why?)

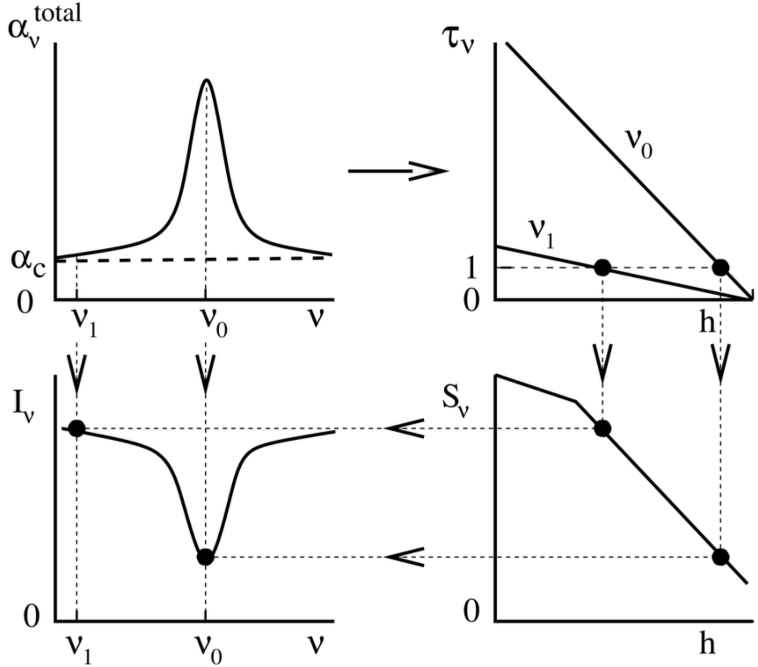

SIMPLE EMISSION LINE

- extinction: bb process gives peak in $\alpha_{\rm total} = \alpha_c + \alpha_l = (1 + \eta_\nu)\,\alpha_c$
- optical depth: assume height-invariant $\alpha_{\rm total} \Rightarrow$ linear $(1 + \eta_\nu)\,\tau_c$
- source function: assume same for line (bb) and continuous (bf, ff) processes
- use Eddington-Barbier (here nearly exact, why?)

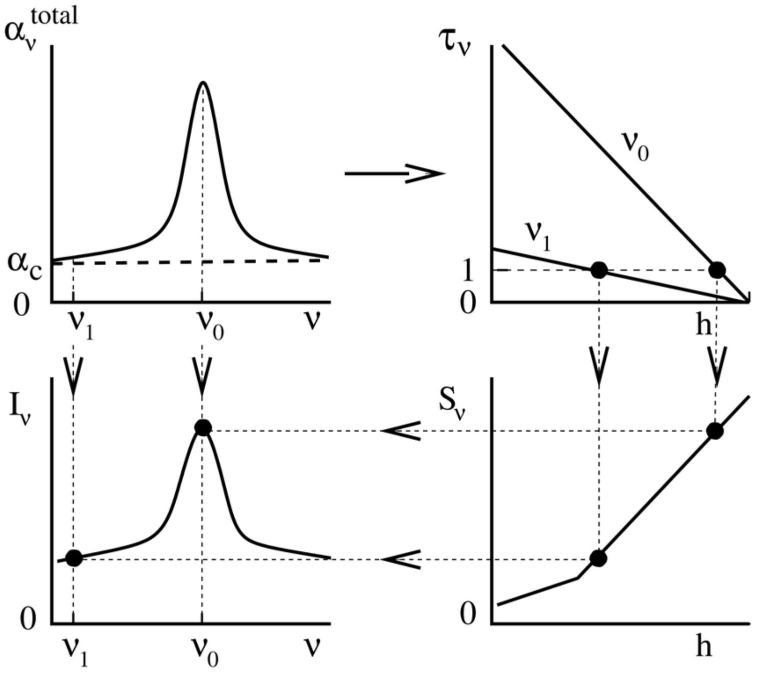

SIMPLE ABSORPTION EDGE

- extinction: bf process gives edge in α_ν^c, with $\alpha_\nu^c \propto \nu^3$ if hydrogenic
- optical depth: assume height-invariant (unrealistic, why?)
- source function: assume same for the whole frequency range (unrealistic, why?)
- use Eddington-Barbier (here nearly exact, why?)

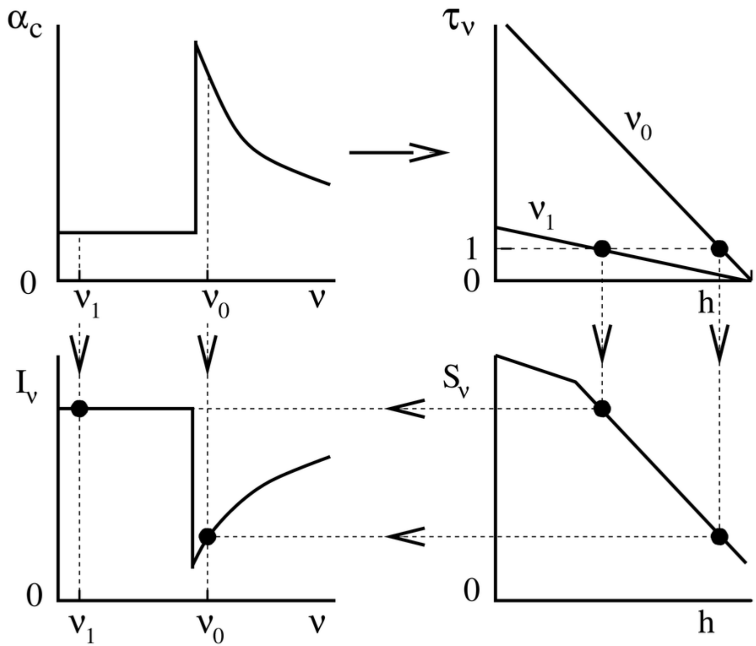

SIMPLE EMISSION EDGE

- extinction: bf process gives edge in α_ν^c, with $\alpha_\nu^c \propto \nu^3$ if hydrogenic
- optical depth: assume height-invariant (unrealistic, why?)
- source function: assume same for the whole frequency range (unrealistic, why?)
- use Eddington-Barbier (here nearly exact, why?)

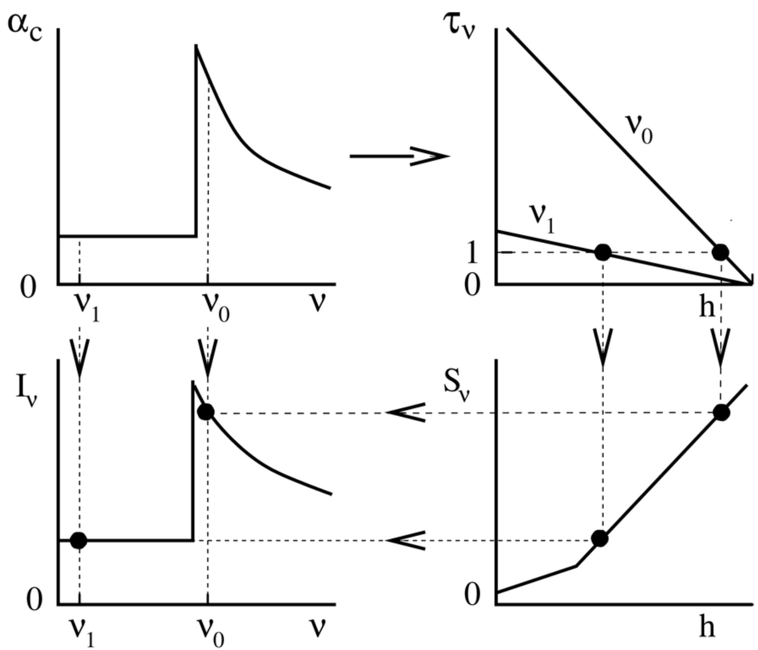

SELF-REVERSED ABSORPTION LINE

- extinction: bb peak with height-dependent amplitude and shape
- optical depth: non-linear even in the log
- source function: decrease followed by increase (any idea why?)
- use Eddington-Barbier (questionable, why?)

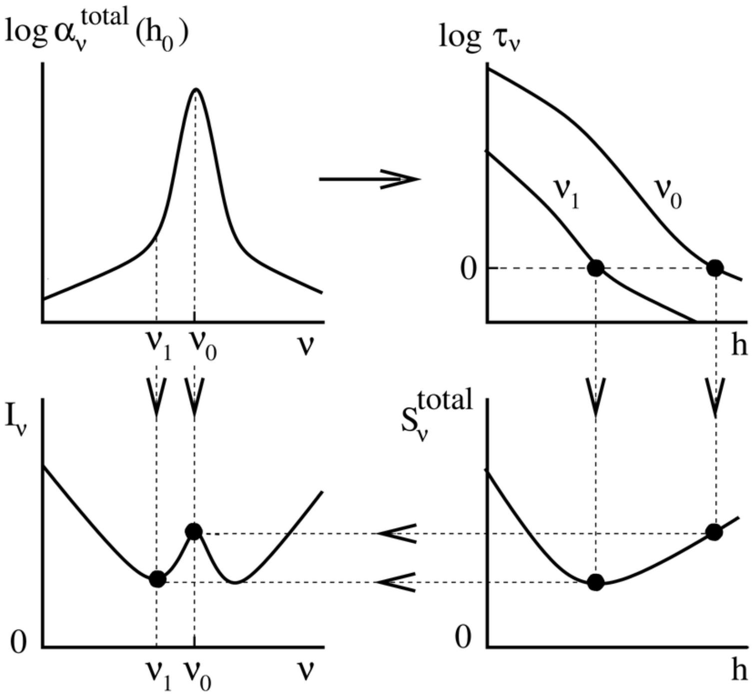

DOUBLY REVERSED ABSORPTION LINE

- extinction: bb peak with height-dependent amplitude and shape
- optical depth: non-linear even in the log
- source function: decrease followed by increase followed by decrease (any idea why?)
- use Eddington-Barbier (questionable, why?)

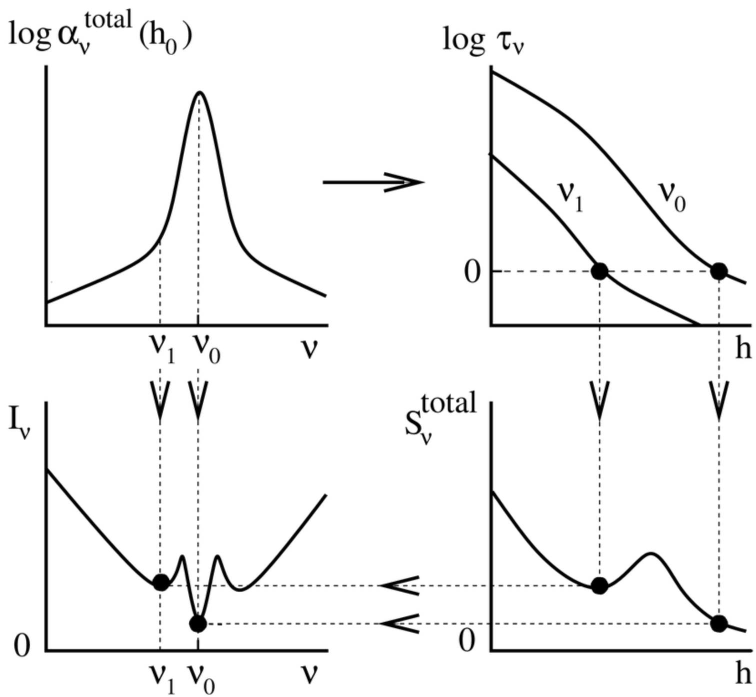

DOUBLY REVERSED ABSORPTION LINE

- extinction: bb peak with height-dependent amplitude and shape
- optical depth: non-linear even in the log
- source function: decrease followed by increase followed by decrease (NLTE scattering)
- use Eddington-Barbier (questionable, why?)

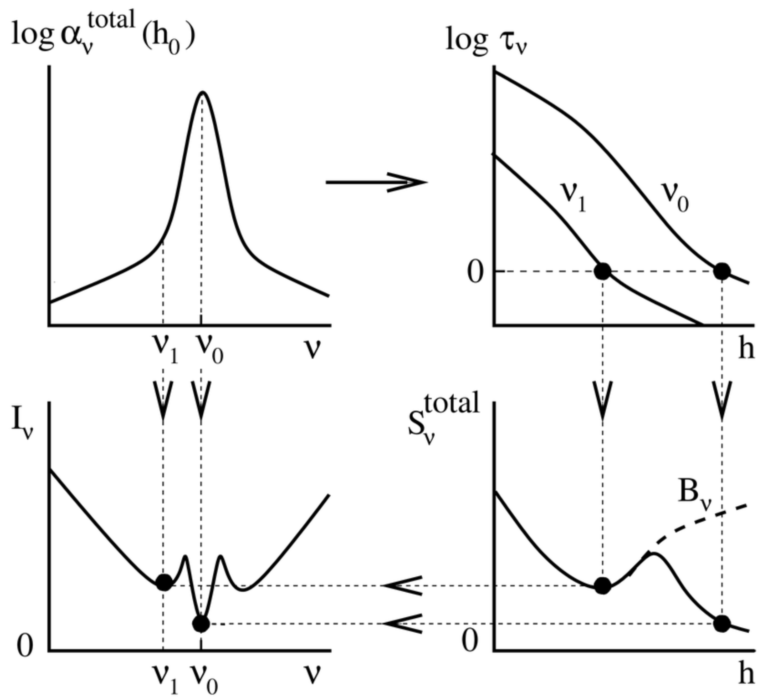

SOLAR SPECTRUM FORMATION

Robert J. Rutten

[Sterrekundig Instituut Utrecht & Institutt for Teoretisk Astrofysikk Oslo]

Texts: R.J. Rutten, *"Radiative Transfer in Stellar Atmospheres"* (RTSA), my website
D. Mihalas, *"Stellar Atmospheres"*, 1970, 1978
G.B. Rybicki and A.P. Lightman, *"Radiative Processes in Astrophysics"*, 1979, 2004
M. Stix, *"The Sun"*, 1989, 2002/2004

examples of local, nonlocal, converted photons: white light corona coronium lines EUV corona EUV bright/dark [Zanstra & Bowen PN lines]

radiative transfer basics: basic quantities constant S_ν plane-atmosphere RT Eddington-Barbier cartoons

LTE 1D solar radiation escape: Planck continuous opacity LTE continuum Boltzmann-Saha LTE line equations LTE line cartoons solar ultraviolet spectrum VALIIIC temperature solar spectrum formation Ca II H&K versus Halpha

NLTE 1D solar radiation escape: bb processes bb rates bb equilibria scattering solar radiation processes VAL3C continuum formation radiative cooling VAL3C radiation budget realistic line cartoon Na D1 Ca II 8542 versus Halpha

MHD-simulated essolar radiation escape: Ca II H in 1D Na D1 in 3D non-E hydrogen in 2D

summary: RTSA rap

PLANCK

RTSA Chapt. 2; Stix 4.5

Planck function in intensity units

$$B_\nu(T) = \frac{2h\nu^3}{c^2}\frac{1}{e^{h\nu/kT}-1} \qquad B_\lambda(T) = \frac{2hc^2}{\lambda^5}\frac{1}{e^{hc/\lambda kT}-1} \qquad B_\sigma(T) = 2hc^2\sigma^3\frac{1}{e^{hc\sigma/kT}-1}$$

Approximations

Wien: $B_\nu(T) \approx \frac{2h\nu^3}{c^2}\,e^{-h\nu/kT}$ Rayleigh-Jeans: $B_\nu(T) \approx \frac{2\nu^2 kT}{c^2}$

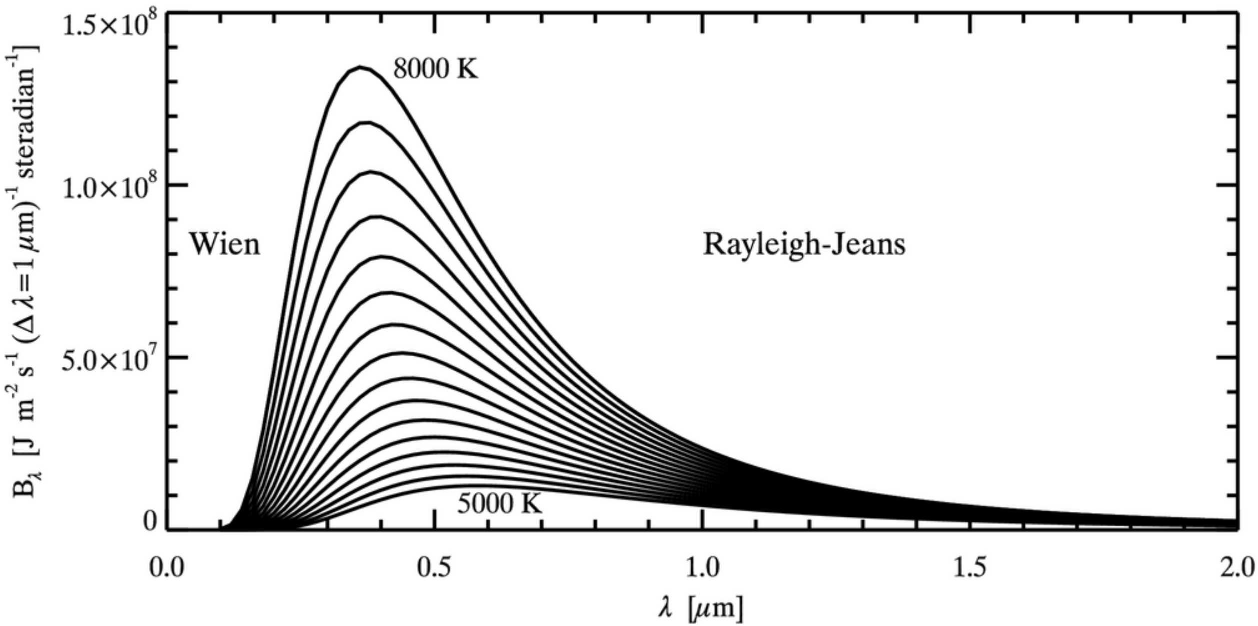

PLANCK FUNCTION VARIATIONS

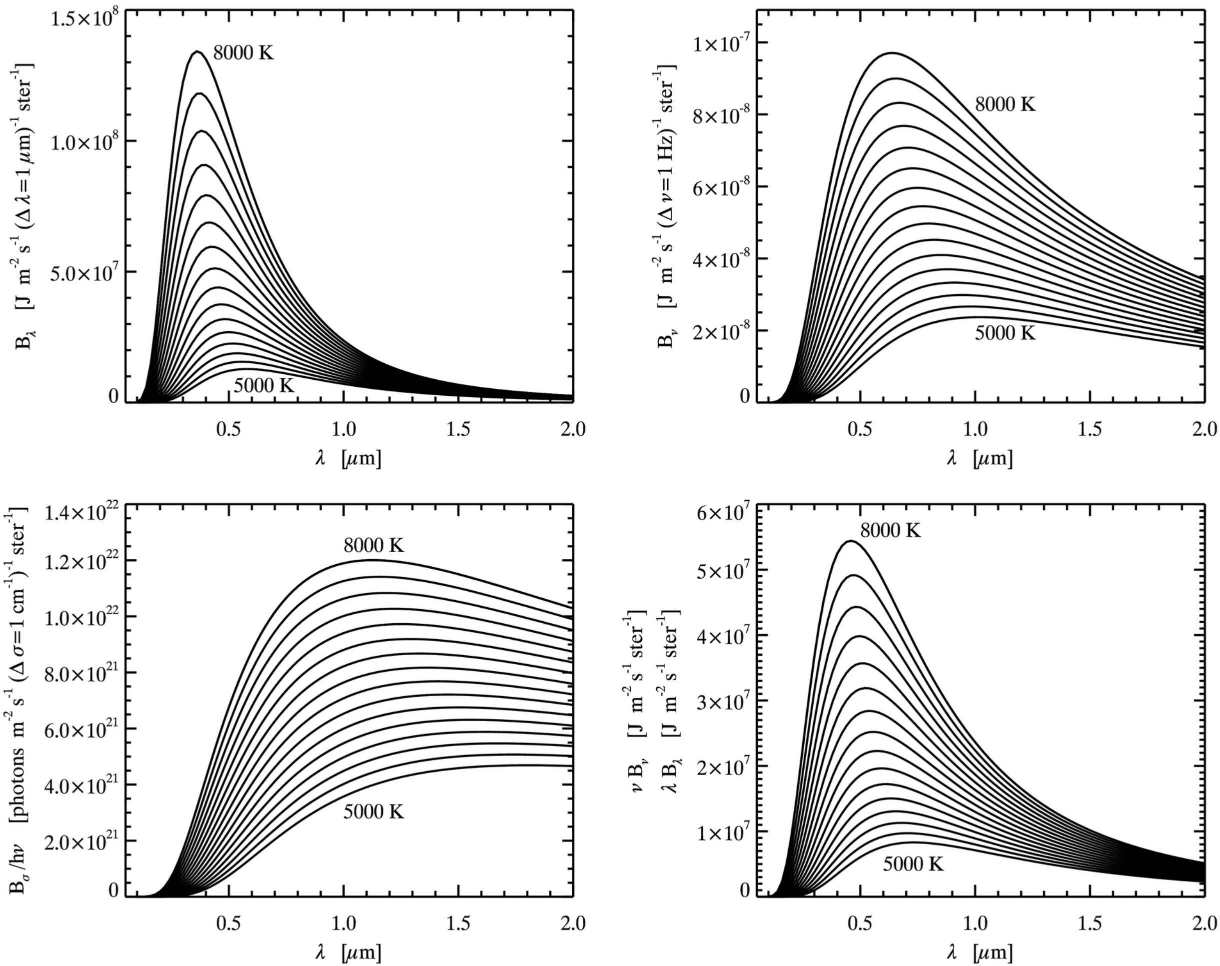

CONTINUOUS OPACITY IN THE SOLAR PHOTOSPHERE

RTSA Chapt. 8; Stix Fig. 4.5; figure from E. Böhm-Vitense

- *bound-free*
  - optical, near-infrared: H^-
  - UV: Si I, Mg I, Al I, Fe I
    (electron donors for H^-)
  - EUV: H I Lyman; He I, He II
- *free-free*
  - infrared, sub-mm: H^-
  - radio: H I
- *electron scattering*
  - Thomson scattering (large height)
  - Rayleigh scattering (near-UV)
- *Rosseland average*

$$\frac{1}{\overline{\kappa}} = \int_0^\infty \frac{1}{\kappa_\nu} \, \frac{\mathrm{d}B_\nu/\mathrm{d}T}{\mathrm{d}B/\mathrm{d}T} \, \mathrm{d}\nu$$

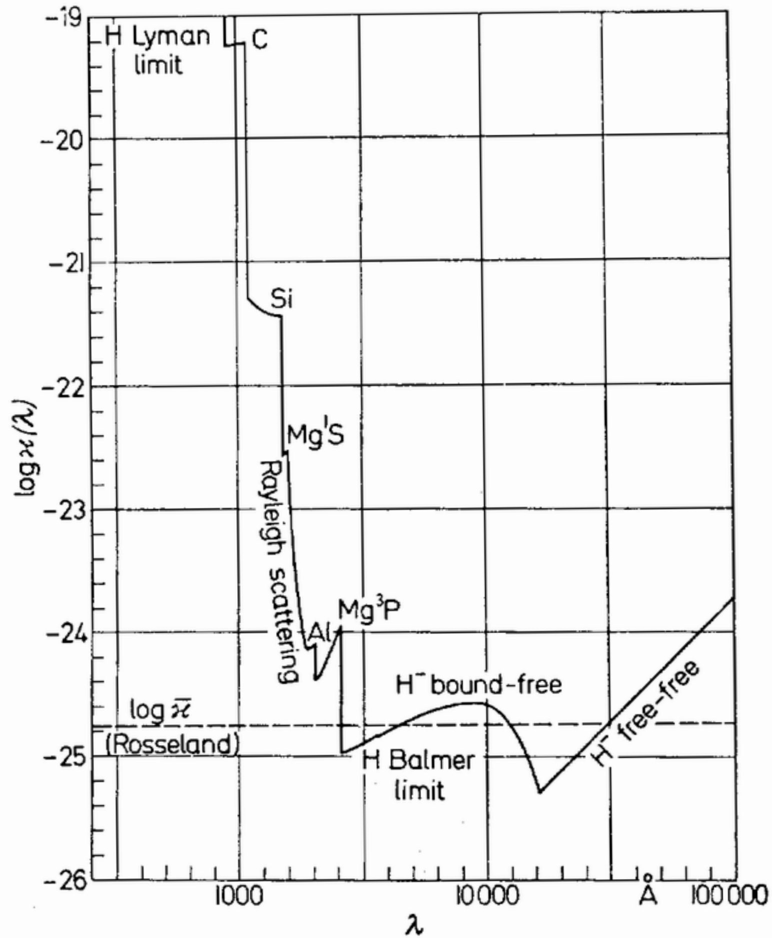

SOLAR OPTICAL AND NEAR-INFRARED CONTINUUM FORMATION

Assumed: LTE, opacity only from H I bf+ff and H^- bf+ff, FALC model atmosphere
Solar disk-center continuum: from Allen, *"Astrophysical Quantities"*, 1976

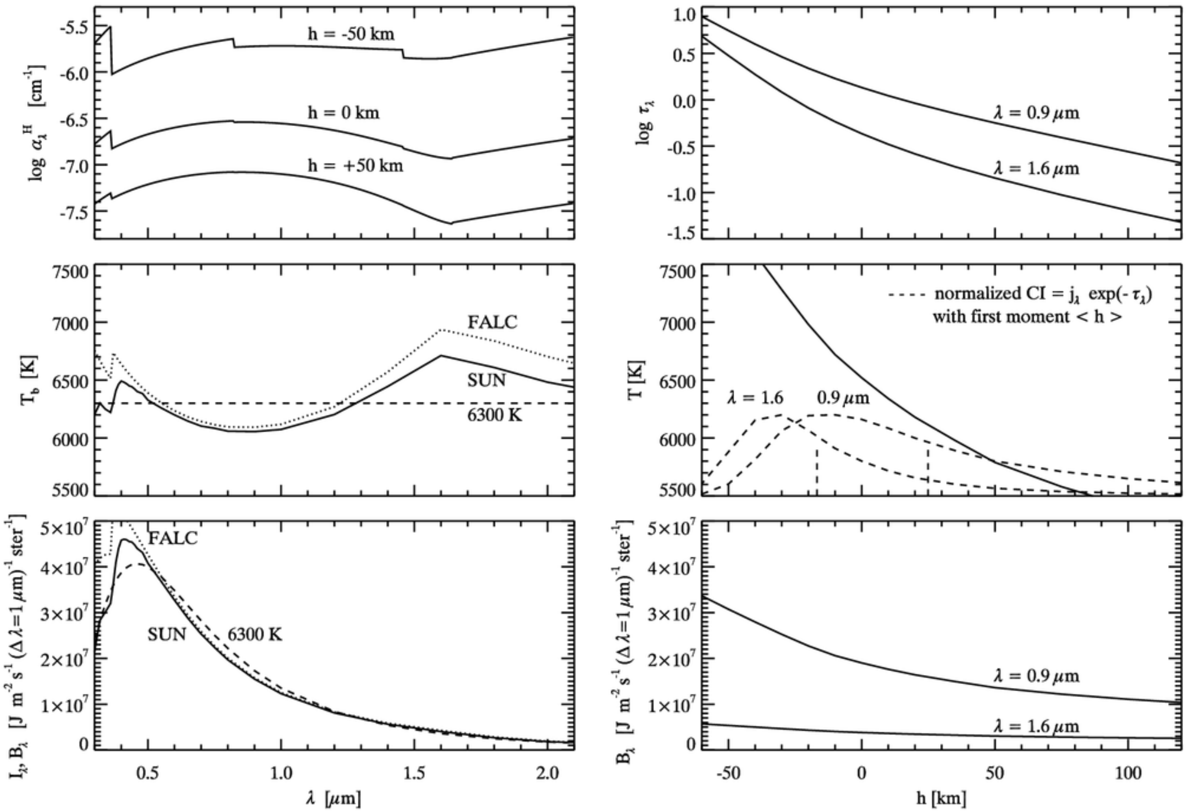

Does the Eddington-Barbier approximation hold?

Saha–Boltzmann level populations

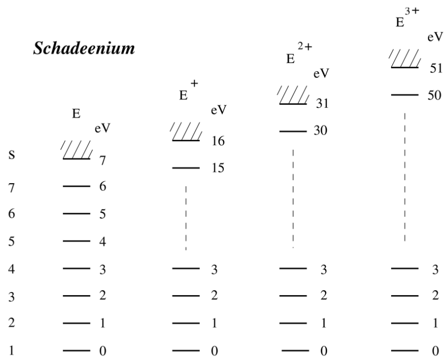

Boltzmann distribution per ionization stage: $\frac{n_{r,s}}{N_r} = \frac{g_{r,s}}{U_r}\, \mathrm{e}^{-\chi_{r,s}/kT}$

partition function: $U_r \equiv \sum_s g_{r,s}\, \mathrm{e}^{-\chi_{r,s}/kT}$

Saha distribution over ionization stages:

$$\frac{N_{r+1}}{N_r} = \frac{1}{N_\mathrm{e}} \frac{2\, U_{r+1}}{U_r} \left(\frac{2\pi m_\mathrm{e} kT}{h^2}\right)^{3/2} \mathrm{e}^{-\chi_r/kT}$$

Saha–Boltzmann Schadeenium

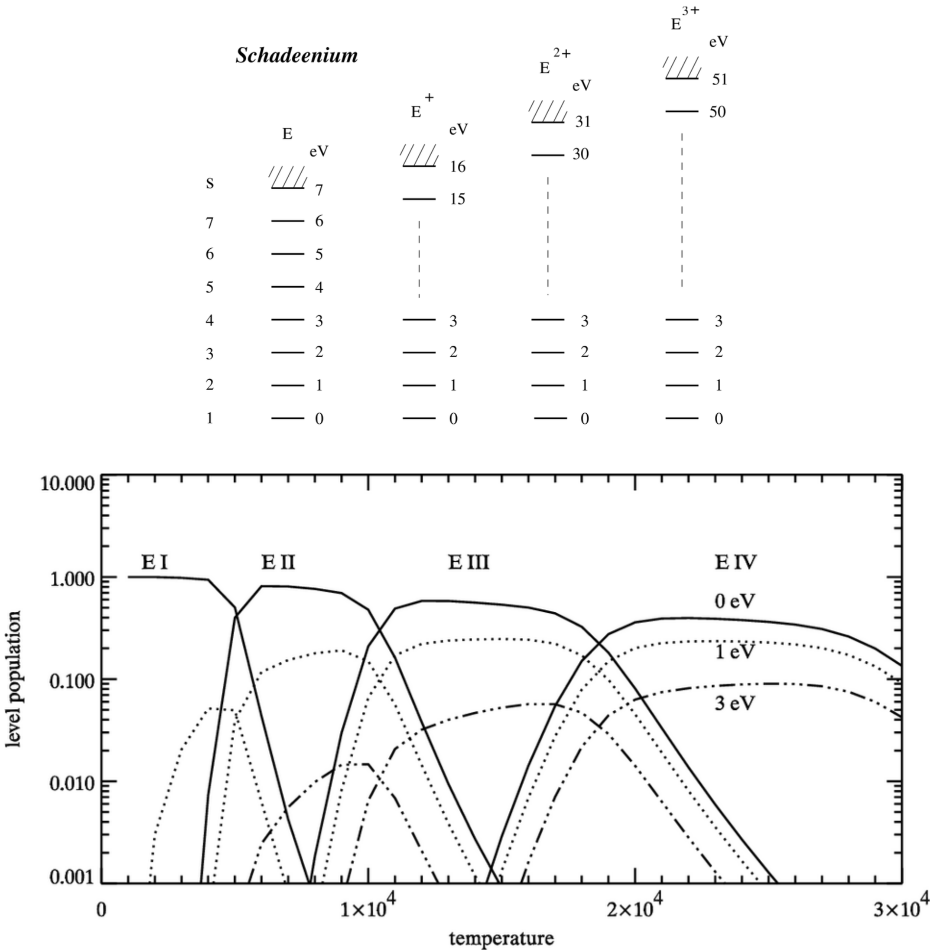

LTE LINES

RTSA Chapt. 2; Stix 4.1.3

continuum optical depth scale

$$\eta_\nu \equiv \kappa_l / \kappa_C \qquad \mathrm{d}\tau_\nu = \mathrm{d}\tau_C + \mathrm{d}\tau_l = (1+\eta_\nu)\,\mathrm{d}\tau_C$$

emergent intensity at disk center in LTE

$$I_\nu(0,1) = \int_0^\infty B_\nu\,\exp(-\tau_\nu)\,\mathrm{d}\tau_\nu = \int_0^\infty (1+\eta_\nu)\,B_\nu\,\exp\left(-\int_0^{\tau_C}(1+\eta_\nu)\,\mathrm{d}\tau'_C\right)\,\mathrm{d}\tau_C$$

Eddington-Barbier: $I_\nu(0,1) \approx B_\nu\,[\tau_\nu\!=\!1] = B_\nu\,[\tau_C\!=\!1/(1\!+\!\eta_\nu)]$

line extinction coefficient shape = Maxwell [+ "microturbulence"] Gauss ⊗ damping Lorentz

$$\Delta\nu_\mathrm{D} \equiv \frac{\nu_0}{c}\sqrt{\frac{2RT}{A}\;[+\xi_\mathrm{t}^2]} \qquad \phi(\nu) = \frac{\gamma}{\sqrt{\pi}\Delta\nu_\mathrm{D}}\int_{-\infty}^{+\infty}\frac{\exp(-(\nu-\nu')^2/\Delta\nu_\mathrm{D}^2)}{[2\pi(\nu'-\nu_0)]^2+\gamma^2/4}\,\mathrm{d}\nu' = \frac{1}{\sqrt{\pi}\Delta\nu_\mathrm{D}}\,H(a,v)$$

Voigt function

$$v \equiv \frac{\nu-\nu_0}{\Delta\nu_\mathrm{D}} \qquad a \equiv \frac{\gamma}{4\pi\Delta\nu_\mathrm{D}} \qquad H(a,v) \equiv \frac{a}{\pi}\int_{-\infty}^{+\infty}\frac{\mathrm{e}^{-y^2}}{(v-y)^2+a^2}\,\mathrm{d}y$$

area in v: $\sqrt{\pi}$

line extinction coefficient

$$\sigma_l = \frac{h\nu}{4\pi}\,B_{lu}\,\phi(\nu) = \frac{\pi e^2}{m_\mathrm{e}c}\,f_l\,\phi(\nu) = \frac{\sqrt{\pi}\,e^2\,f_l}{m_\mathrm{e}c\,\Delta\nu_\mathrm{D}}\,H(a,v) \qquad A_{ul} = 6.67\times10^{13}\,\frac{g_l}{g_u}\,\frac{f_{lu}}{\lambda^2}\;\mathrm{s}^{-1}\,(\lambda\;\mathrm{nm})$$

$$\kappa_l = \sigma_l\,n_l^\mathrm{LTE}\,(1-\mathrm{e}^{-h\nu/kT})/\rho = \frac{\sigma_l}{\mu m_\mathrm{H}}\,\frac{n_i}{\sum n_i}\,\frac{n_{ij}}{n_i}\,\frac{n_{ijk}}{n_{ij}}\,(1-\mathrm{e}^{-h\nu/kT})$$

i, j, k species, stage, lower level
abundance, Saha, Boltzmann

STELLAR LTE ABSORPTION LINE

- extinction: large bb peak in $\alpha_{\rm total}(h) = \alpha_c(h) + \alpha_l(h)$, both decreasing with height
- optical depth: the inward integration $\tau_\nu = -\int \alpha_\nu \, {\rm d}h$ along the line of sight reaches $\tau_\nu = 1$ at much larger height at line center than in the adjacent continuum
- source function: $S_\nu(h) = B_\nu[T(h)]$ (neglect variation over the profile)
- intensity: the emergent profile is a two-sided mapping of $B_\nu[T(h)]$ sampled at $h(\tau_\nu \approx 1)$

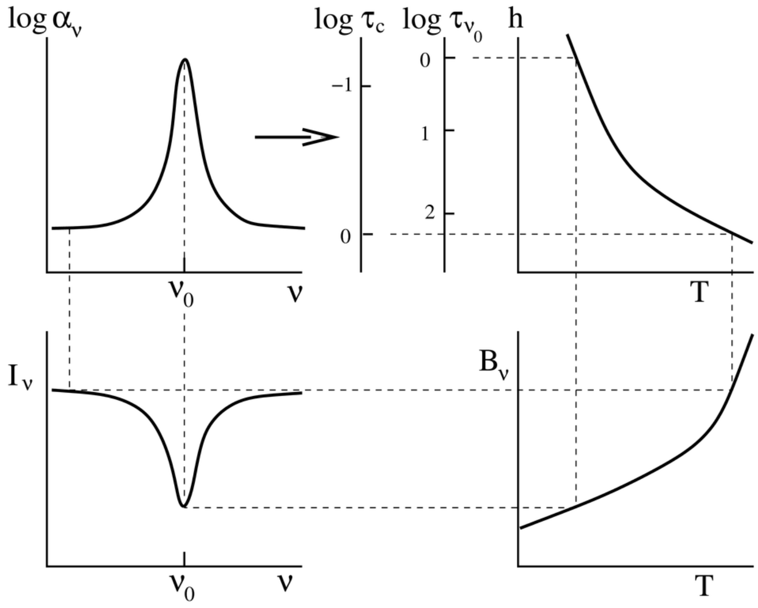

Why are LTE lines with the same $\alpha_c(h)$ and $\alpha_l(h)$ deeper in the blue than in the red?

STELLAR LTE SELF-REVERSED LINE

- extinction: large bb peak in $\alpha_{\rm total}(h) = \alpha_c(h) + \alpha_l(h)$, both decreasing with height
- optical depth: the inward integration $\tau_\nu = -\int \alpha_\nu \, {\rm d}h$ along the line of sight reaches $\tau_\nu = 1$ at much larger height at line center than in the adjacent continuum
- source function: $S_\nu(h) = B_\nu[T(h)]$ (neglect variation over the profile)
- intensity: the emergent profile is a two-sided mapping of $B_\nu[T(h)]$ sampled at $h(\tau_\nu \approx 1)$

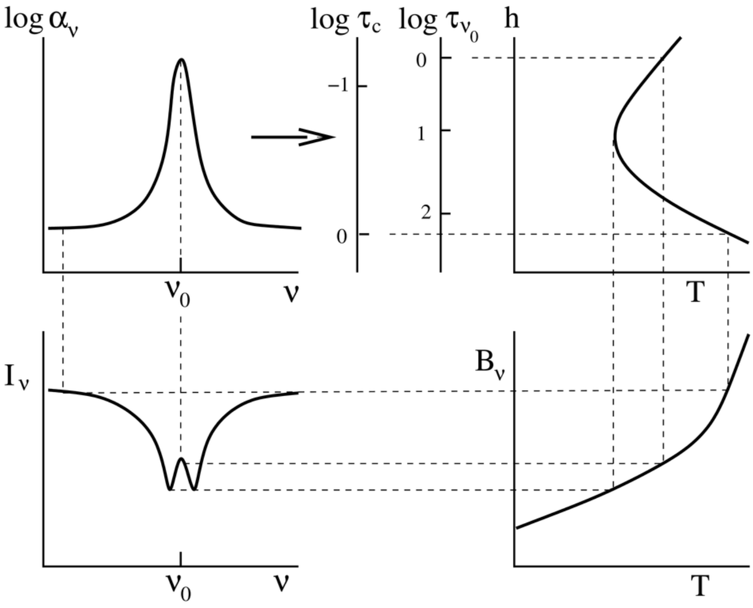

SOLAR ULTRAVIOLET SPECTRUM

Scheffler & Elsässer, courtesy Karin Muglach

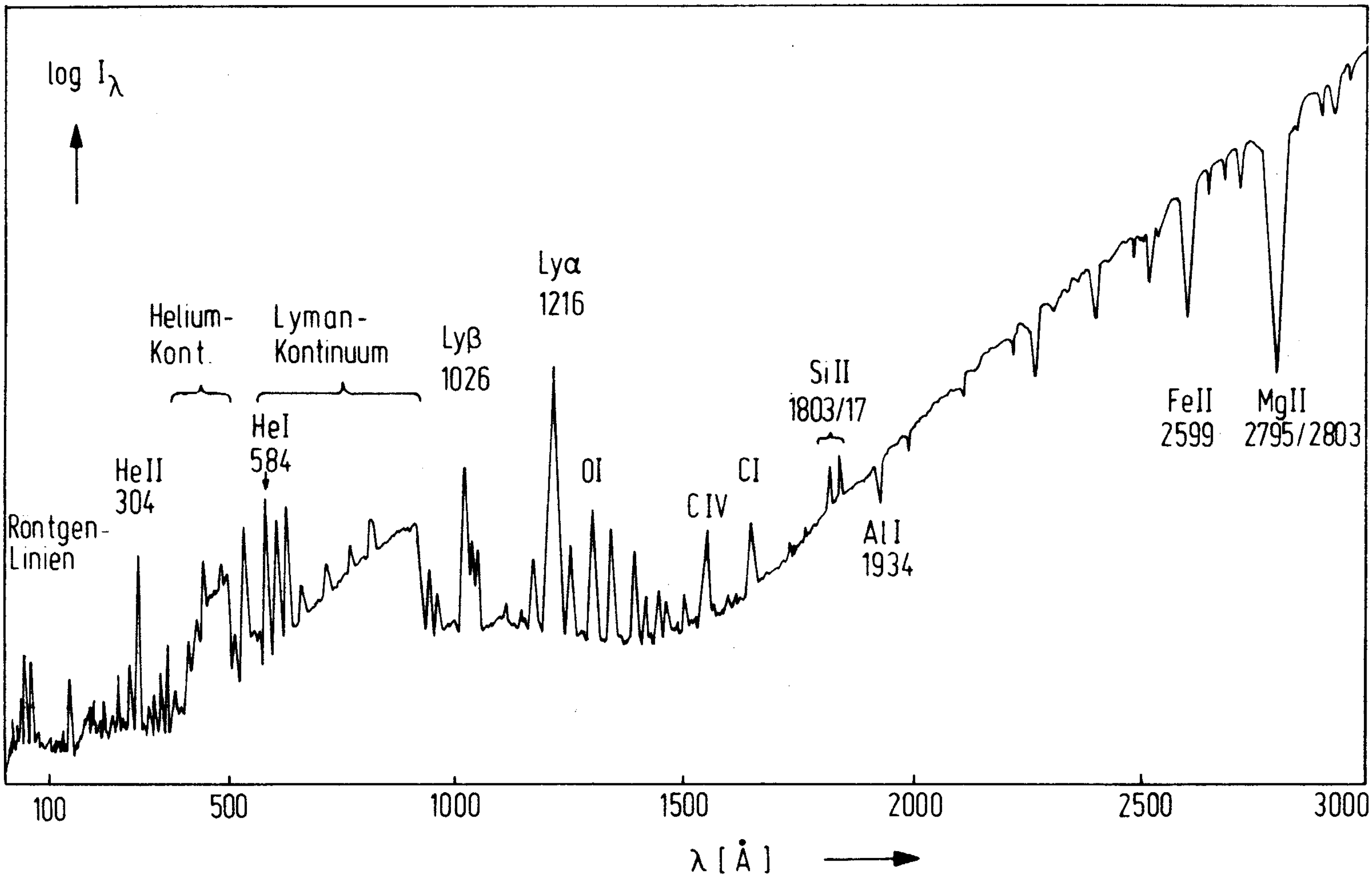

VALIIIC MODEL

Vernazza, Avrett, Loeser 1981ApJS...45..635V

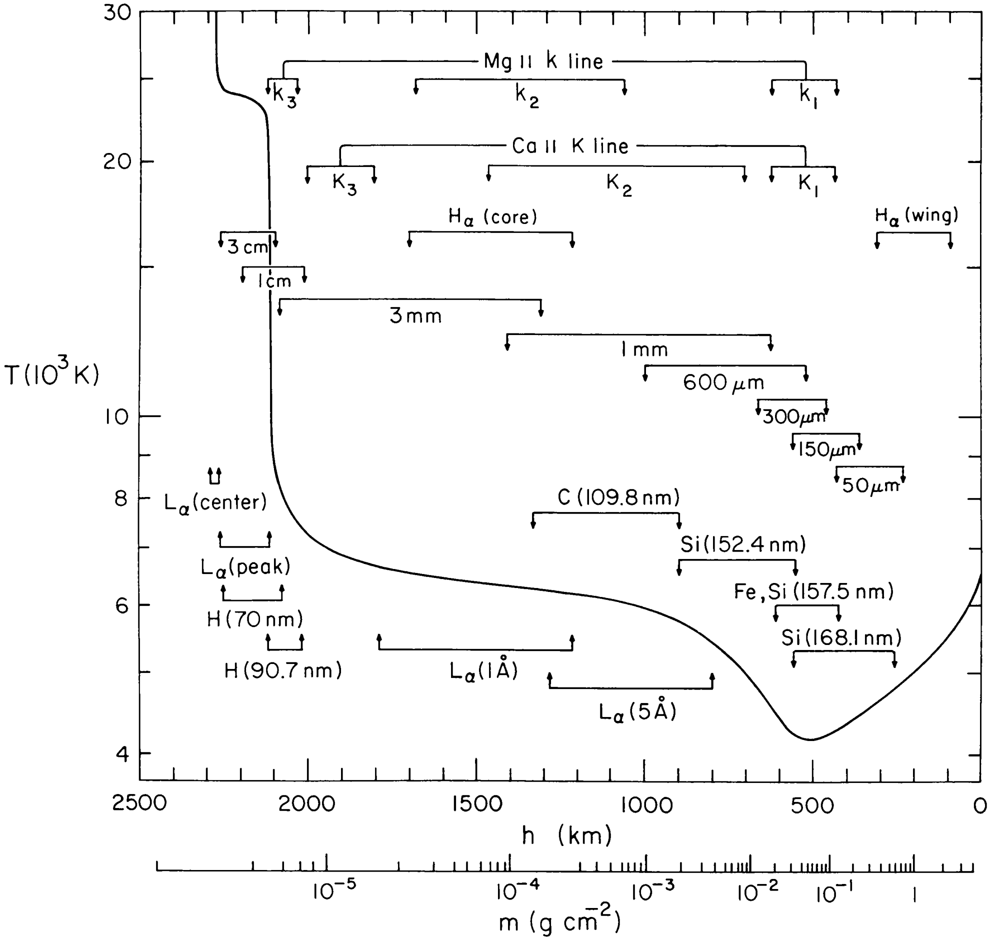

SOLAR SPECTRUM FORMATION

Avrett 1990IAUS..138....3A

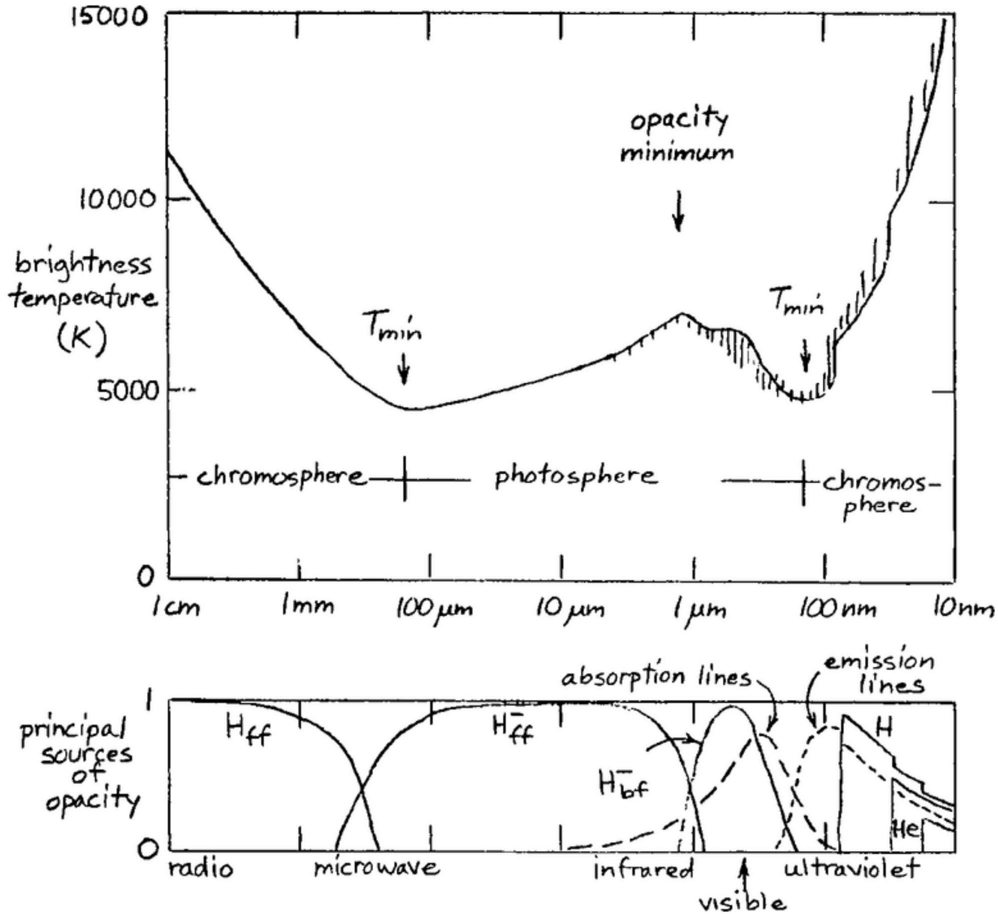

H-α AND Ca II K IN THE SOLAR SPECTRUM

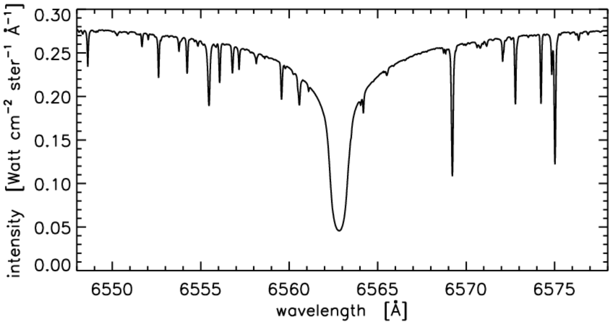

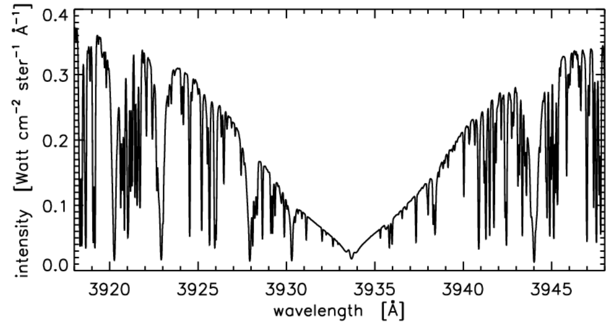

solar abundance ratio: Ca/H = 2×10^{-6}

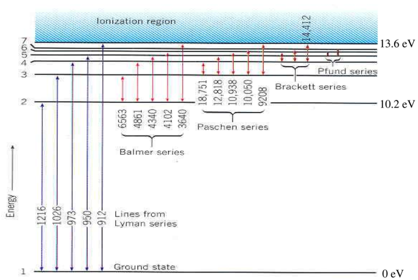

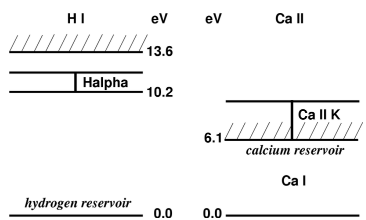

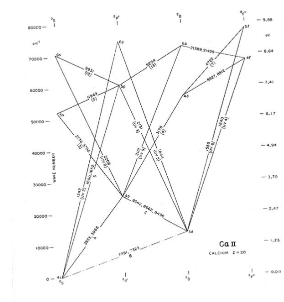

Assuming LTE at $T = 5000\,$K, $P_e = 10^2\,$dyne cm^{-2}:

Boltzmann H I: $\frac{n_2}{n_1} = 4.2 \times 10^{-10}$ Saha Ca II: $\frac{N_{\mathrm{Ca\,II}}}{N_{\mathrm{Ca}}} \approx 1$ $\frac{\text{Ca II}\,(n=1)}{\text{H I}\,(n=2)} = 8 \times 10^3$

Ca II H & Hα in LTE

Leenaarts et al. 2006A&A...449.1209L

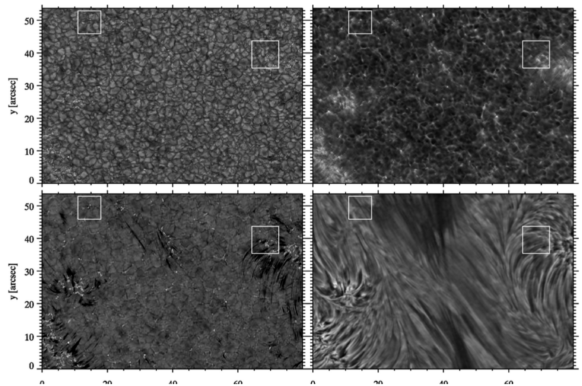

http://dot.astro.uu.nl

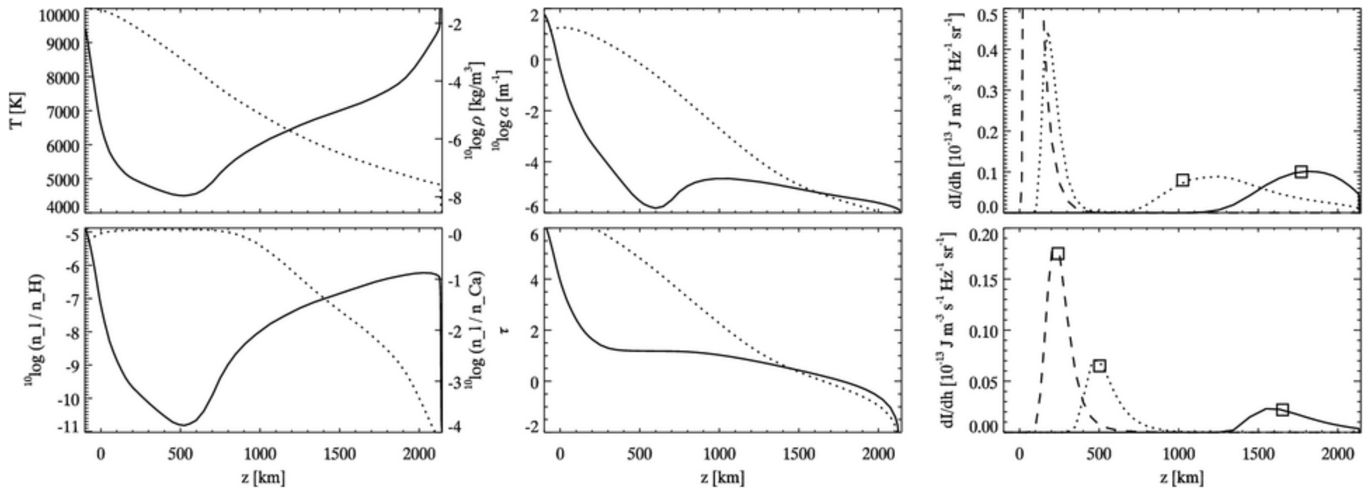

SOLAR SPECTRUM FORMATION

Robert J. Rutten

[Sterrekundig Instituut Utrecht & Institutt for Teoretisk Astrofysikk Oslo]

Texts: R.J. Rutten, *"Radiative Transfer in Stellar Atmospheres"* (RTSA), my website
D. Mihalas, *"Stellar Atmospheres"*, 1970, 1978
G.B. Rybicki and A.P. Lightman, *"Radiative Processes in Astrophysics"*, 1979, 2004
M. Stix, *"The Sun"*, 1989, 2002/2004

examples of local, nonlocal, converted photons: white light corona coronium lines EUV corona EUV bright/dark [Zanstra & Bowen PN lines]

radiative transfer basics: basic quantities constant S_ν plane-atmosphere RT Eddington-Barbier cartoons

LTE 1D solar radiation escape: Planck continuous opacity LTE continuum Boltzmann-Saha LTE line equations LTE line cartoons solar ultraviolet spectrum VALIIIC temperature solar spectrum formation Ca II H&K versus Halpha

NLTE 1D solar radiation escape: bb processes bb rates bb equilibria scattering solar radiation processes VAL3C continuum formation radiative cooling VAL3C radiation budget realistic line cartoon Na D1 Ca II 8542 versus Halpha

MHD-simulated essolar radiation escape: Ca II H in 1D Na D1 in 3D non-E hydrogen in 2D

summary: RTSA rap

BOUND-BOUND PROCESSES AND EINSTEIN COEFFICIENTS

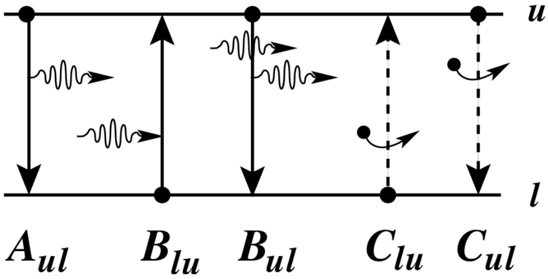

Spontaneous deexcitation

$A_{ul} \equiv$ transition probability for spontaneous deexcitation from state u to state l per sec per particle in state u

Radiative excitation

$B_{lu}\overline{J}^{\varphi}_{\nu_0} \equiv$ number of radiative excitations from state l to state u per sec per particle in state l

Induced deexcitation

$B_{ul}\overline{J}^{\chi}_{\nu_0} \equiv$ number of induced radiative deexcitations from state u to state l per sec per particle in state u

Collisional excitation and deexcitation

$C_{lu} \equiv$ number of collisional excitations from state l to state u per sec per particle in state l

$C_{ul} \equiv$ number of collisional deexcitations from state u to state l per sec per particle in state u

BOUND-BOUND RATES

RTSA 2.3.1, 2.3.2, 2.6.1; Stix 4.2

Monochromatic bb rates expressed in Einstein coefficients (intensity units)

$n_u A_{ul} \chi(\nu)/4\pi$	$n_u B_{ul} I_\nu \psi(\nu)/4\pi$	$n_l B_{lu} I_\nu \phi(\nu)/4\pi$	$n_u C_{ul}$ $\quad$ $n_l C_{lu}$
spontaneous emission	stimulated emission	radiative excitation	collisional (de-)excitation

Einstein relations

$$g_u B_{ul} = g_l B_{lu} \qquad (g_u/g_l) A_{ul} = (2h\nu^3/c^2)\, B_{lu} \qquad C_{ul}/C_{lu} = (g_l/g_u) \exp(E_{ul}/kT)$$

required for TE detailed balancing with $I_\nu = B_\nu$, but hold universally

General line source function

$$j_\nu = \frac{h\nu}{4\pi} n_u\, A_{ul}\, \chi(\nu) \qquad \alpha_\nu = \frac{h\nu}{4\pi} [n_l\, B_{lu} \phi(\nu) - n_u\, B_{ul} \psi(\nu)] \qquad S_l = \frac{n_u\, A_{ul}\, \chi(\nu)}{n_l\, B_{lu} \phi(\nu) - n_u\, B_{ul} \psi(\nu)}$$

Simplified line source function

CRD: $\chi(\nu) = \psi(\nu) = \phi(\nu)$ $\qquad$ $S_l = \dfrac{n_u\, A_{ul}}{n_l\, B_{lu} - n_u\, B_{ul}} = \dfrac{2h\nu^3}{c^2} \dfrac{1}{\dfrac{g_u n_l}{g_l n_u} - 1}$ $\qquad$ Boltzmann: $S_l = B_\nu(T)$

Statistical equilibrium equations for level j

$$n_j \sum_{j \neq i}^{N} R_{ji} = \sum_{j \neq i}^{N} n_j R_{ij} \qquad R_{ji} = A_{ji} + B_{ji} \overline{J_{ji}} + C_{ji} \qquad \overline{J_{ji}} \equiv \frac{1}{4\pi} \int_0^{4\pi} \int_0^{\infty} I_\nu\, \phi(\nu)\, \mathrm{d}\nu\, \mathrm{d}\Omega$$

time-independent population	bb rates per particle in j	total (= mean) mean intensity

BOUND-BOUND EQUILIBRIA

RTSA missing; Stix 4.1.2

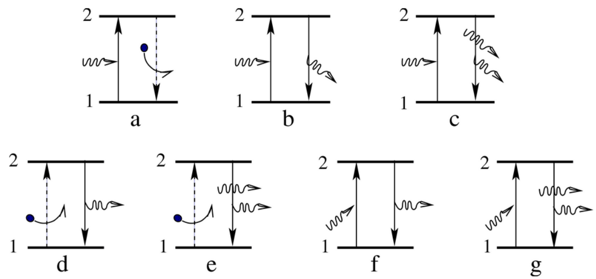

- *LTE = large collision frequency* – interior, low photosphere
  - up: mostly collisional = thermal creation (d + e)
  - down: mostly collisional = large destruction probability (a)
  - photon travel: “honorary gas particles” or negligible leak
- *NLTE = statistical equilibrium or time-dependent* – chromosphere, TR
  - photon travel: non-local impinging (pumping), loss (suction)
  - two-level scattering: coherent/complete/partial redistribution
  - multi-level: photon conversion, sensitivity transcription
- *coronal equilibrium = hot tenuous* – coronal EUV
  - up: only collisional = thermal creation (only d)
  - down: only spontaneous (only d)
  - photon travel: escape / drown / scatter bf H I, He I, He II

SCATTERING EQUATIONS

RTSA 4.1–4.3

Destruction probability

coherent: $\varepsilon_\nu \equiv \dfrac{\alpha^{\rm a}_\nu}{\alpha^{\rm a}_\nu + \alpha^{\rm s}_\nu}$ 2-level CRD: $\varepsilon_{\nu_0} \equiv \dfrac{\alpha^{\rm a}_{\nu_0}}{\alpha^{\rm a}_{\nu_0} + \alpha^{\rm s}_{\nu_0}} = \dfrac{C_{21}}{C_{21} + A_{21} + B_{21} B_{\nu_0}}$

Elastic scattering

coherent: $S_\nu = (1-\varepsilon_\nu) J_\nu + \varepsilon_\nu B_\nu$ 2-level CRD: $S_{\nu_0} = (1-\varepsilon_{\nu_0}) J_{\nu_0} + \varepsilon_{\nu_0} B_{\nu_0}$

Schwarzschild equation and Lambda operator

$$J_\nu(\tau_\nu) \equiv \frac{1}{2}\int_{-1}^{+1} I_\nu(\tau_\nu,\mu)\,{\rm d}\mu = \frac{1}{2}\int_0^\infty S_\nu(t_\nu)\,E_1(|t_\nu - \tau_\nu|)\,{\rm d}t_\nu \equiv \mathbf{\Lambda}_{\tau_\nu}[S_\nu(t_\nu)]$$

surface: $J_\nu(0) \approx \frac{1}{2} S_\nu(\tau_\nu = 1/2)$ depth: $J_\nu(\tau_\nu) \approx S_\nu(\tau_\nu)$ diffusion: $J_\nu(\tau_\nu) \approx B_\nu(\tau_\nu)$

Scattering in an isothermal atmosphere

coherent: $S_\nu(0) = \sqrt{\varepsilon_\nu}\, B_\nu$ 2-level CRD: $S_{\nu_0}(0) = \sqrt{\varepsilon_{\nu_0}}\, B_{\nu_0}$

Thermalizaton depth

coherent: $\Lambda_\nu = 1/\varepsilon_\nu^{1/2}$ Gauss profile: $\Lambda_{\nu_0} \approx 1/\varepsilon_{\nu_0}$ Lorentz profile: $\Lambda_{\nu_0} \approx 1/\varepsilon_{\nu_0}^2$

EXPONENTIAL INTEGRALS

RTSA figure 4.1

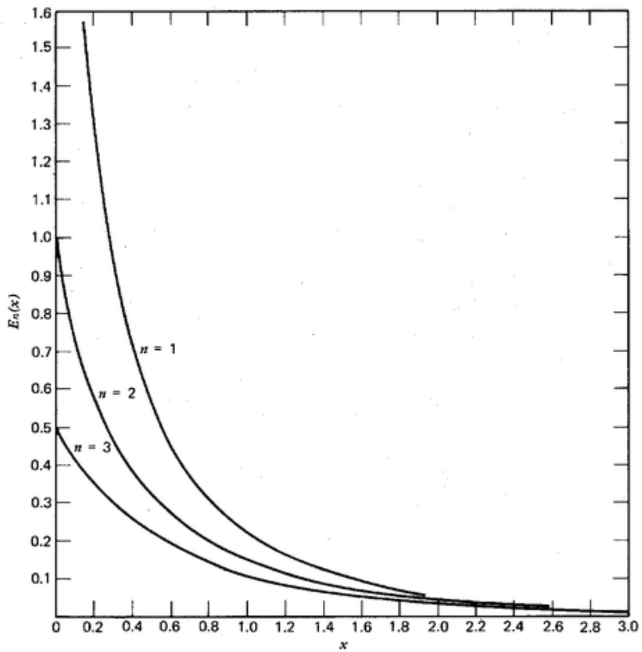

Figure 4.1: The first three exponential integrals $E_n(x)$. $E_1(x)$ has a singularity at $x = 0$. For large x all $E_n(x)$ have $E_n(x) \approx \exp(-x)/x$. From Gray (1992).

THE WORKING OF THE LAMBDA OPERATOR

RTSA figure 4.1; Thijs Krijger production

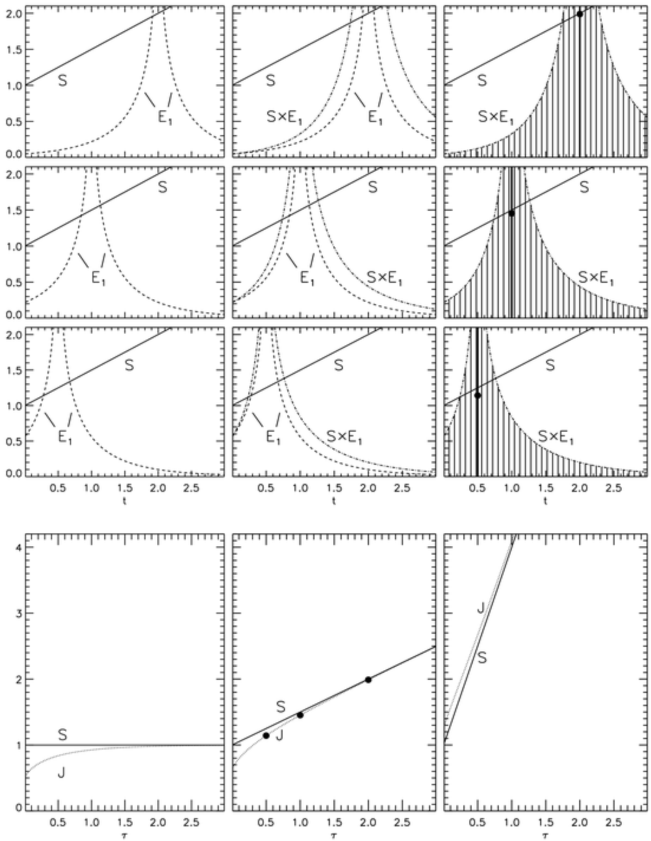

GREY RE LTE SOLAR-TEMPERATURE ATMOSPHERE

RTSA figure 4.9; Thijs Krijger production

Temperature stratification: $T(\tau) \approx T_{\rm eff} \left(\frac{3}{4}\tau + \frac{1}{2}\right)^{1/4}$

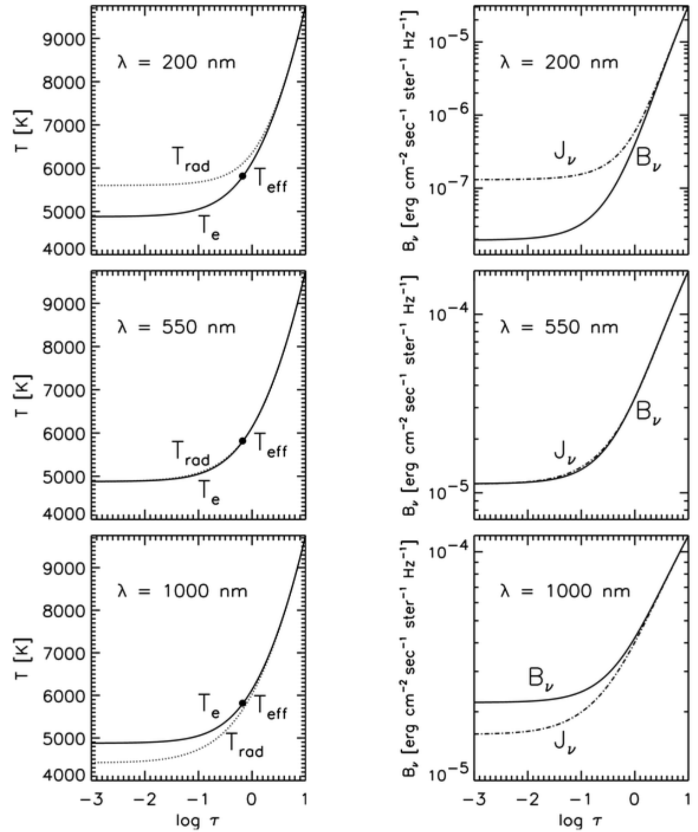

B, J, S FOR SOLAR-LIKE COHERENT LINE SCATTERING

RTSA figure 4.11; Thijs Krijger production

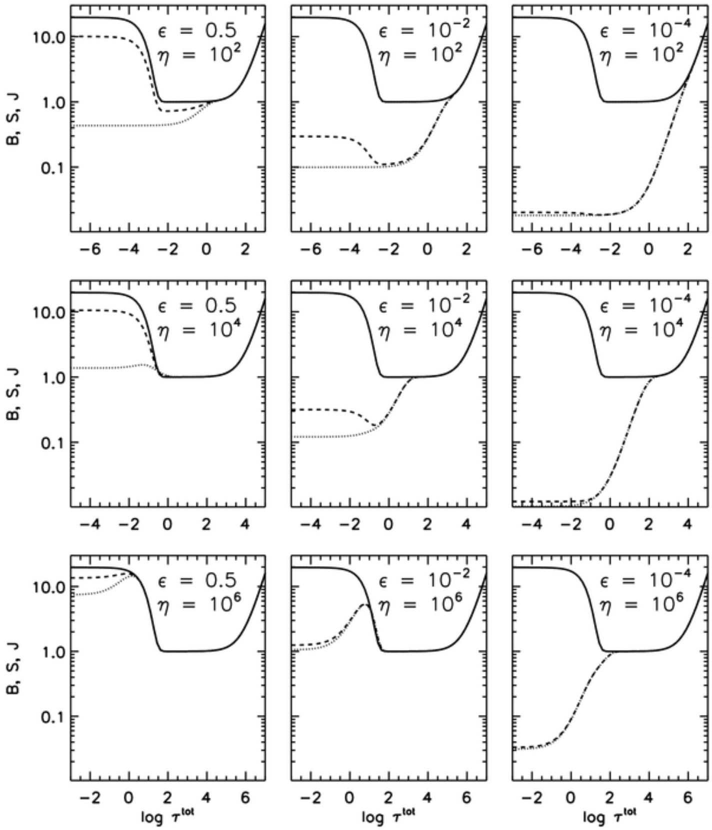

CRD RESONANT SCATTERING IN AN ISOTHERMAL ATMOSPHERE

RTSA figure 4.12; from Avrett 1965SAOSR.174..101A

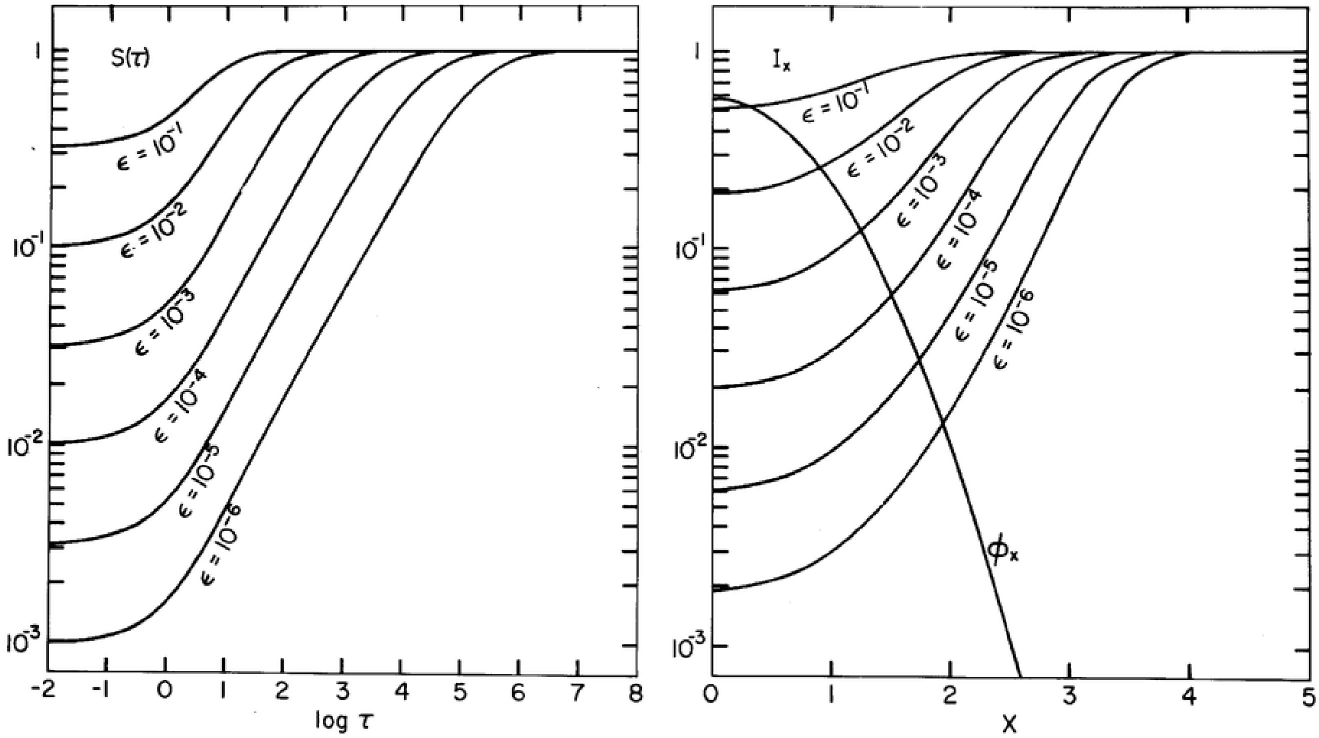

IDEM FOR DIFFERENT LINE PROFILES

RTSA figure 4.12; from Avrett 1965SAOSR.174..101A

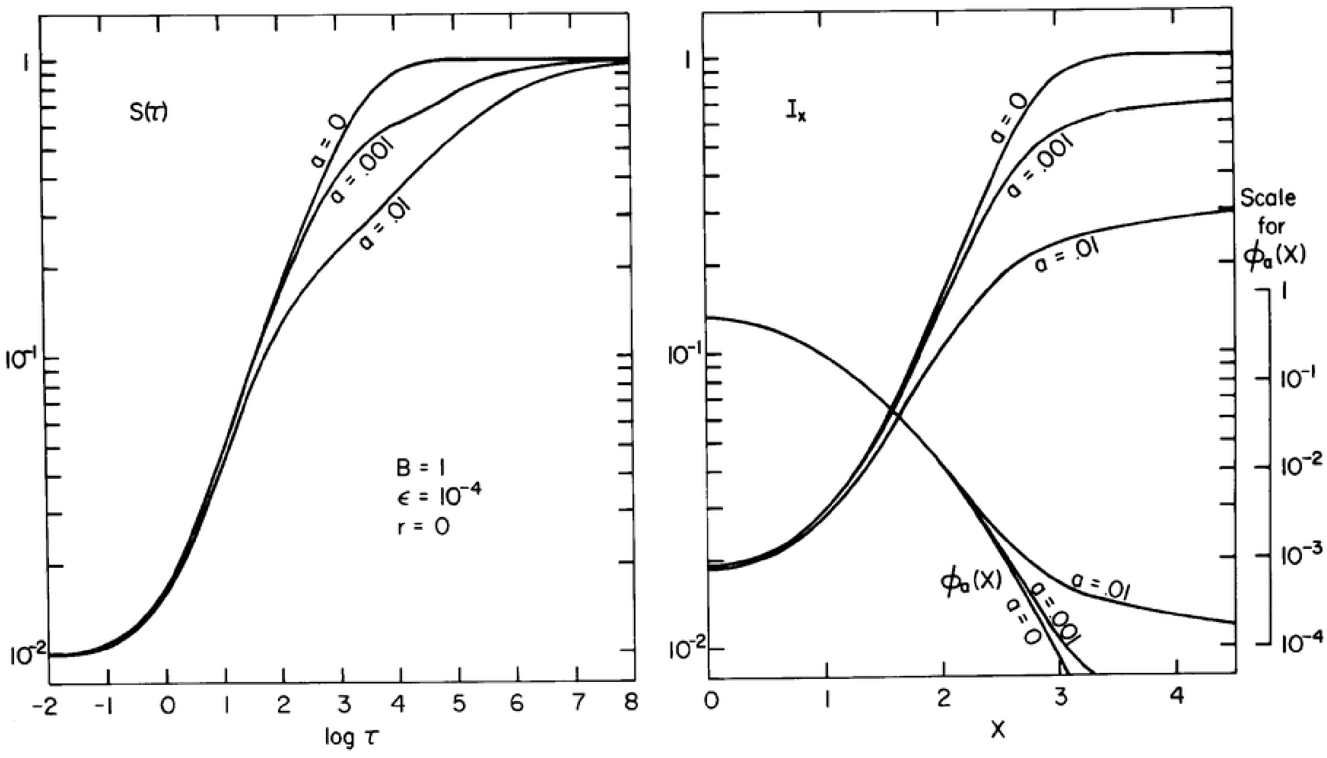

IDEM WITH BACKGROUND CONTINUUM

RTSA figure 4.13; from Avrett 1965SAOSR.174..101A

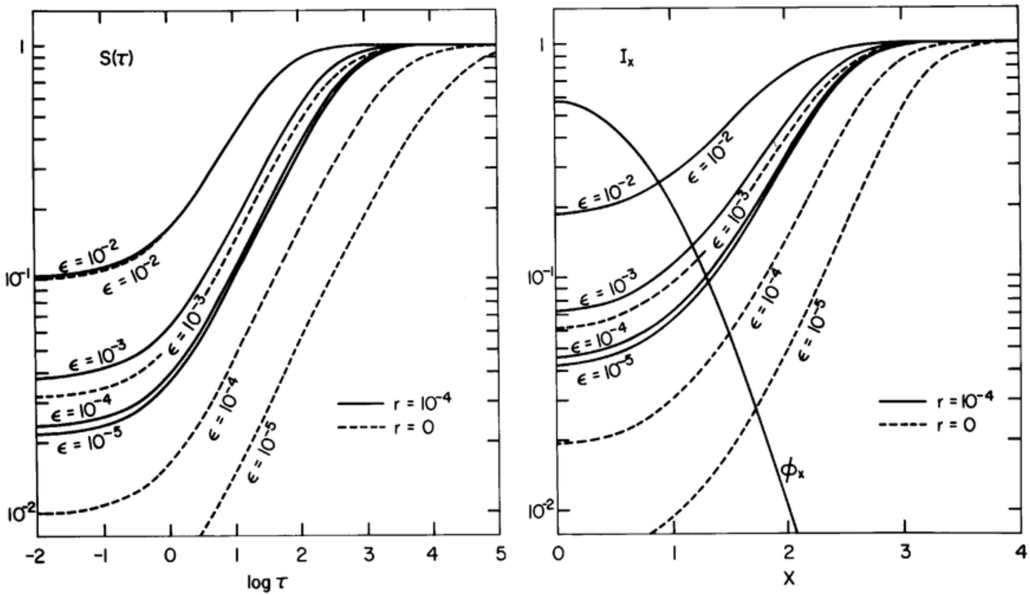

Figure 4.13: Avrett results for two-level-atom lines with complete redistribution and a background continuum. The atmosphere is isothermal. Axis labeling and parameters as for the upper panels of Figure 4.12; the extinction profile $\varphi(x)$ is again Gaussian (righthand panel). *Dashed curves:* $r \equiv \alpha^c_\nu/\alpha^l_{\nu_0}$ set to $r = 0$, describing pure resonance scattering without background continuum. *Solid curves:* $r = 10^{-4}$ or $\eta_{\nu_0} = 10^4$, describing fairly strong lines. Lack of continuum thermalization is unimportant when $r \ll \varepsilon_{\nu_0}$. Lack of collisional destruction is unimportant when $\varepsilon_{\nu_0} \ll r$. From Avrett (1965).

SOLAR ATMOSPHERE RADIATIVE PROCESSES

RTSA Chapt. 8; Stix Fig. 4.5

- *bound-bound* – S_ν, κ_ν NLTE? PRD?
  - neutral atom transitions
  - ion transitions
  - molecule transitions
- *bound-free* – S_ν, κ_ν NLTE? always CRD
  - H^- optical, near-infrared
  - H I Balmer, Lyman; He I, He II
  - Fe I, Si I, Mg I, Al I electron donors
- *free-free* – S_ν always LTE, κ_ν NLTE
  - H^- infrared, sub-mm
  - H I radio
- *electron scattering* – always NLTE, Doppler?
  - Thomson scattering
  - Rayleigh scattering
- *collective* – p.m.
  - cyclotron, synchrotron radiation
  - plasma radiation

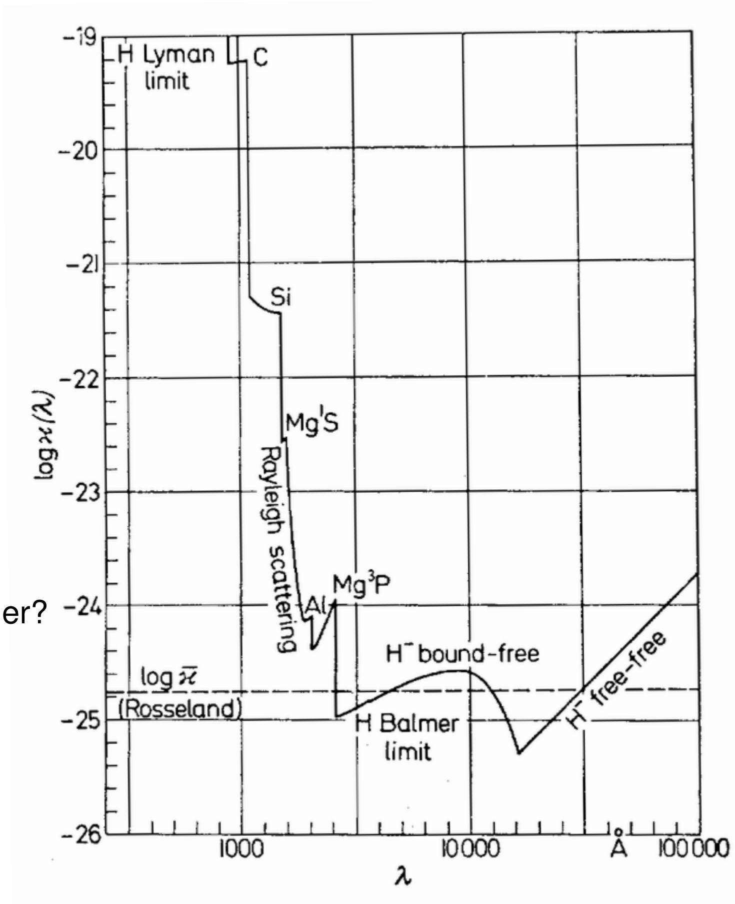

VALIIIC MODEL

Vernazza, Avrett, Loeser   1981ApJS...45..635V

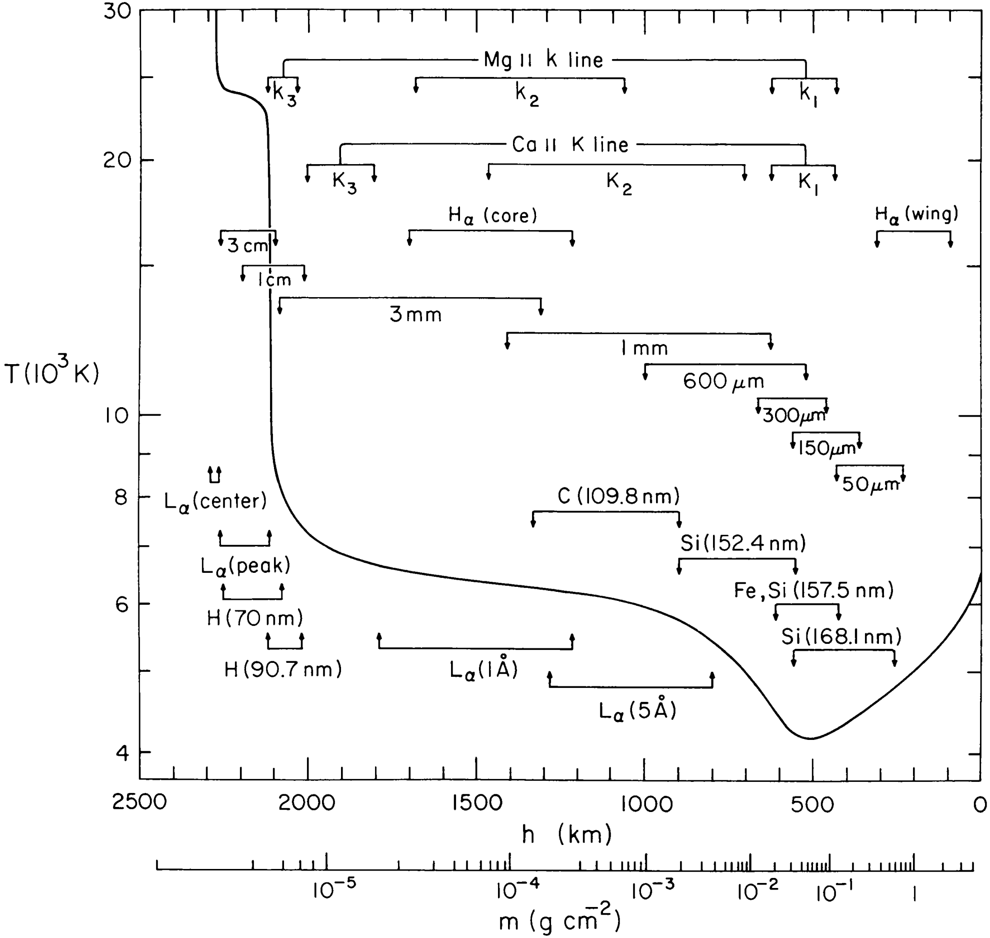

VAL3C CONTINUUM FORMATION

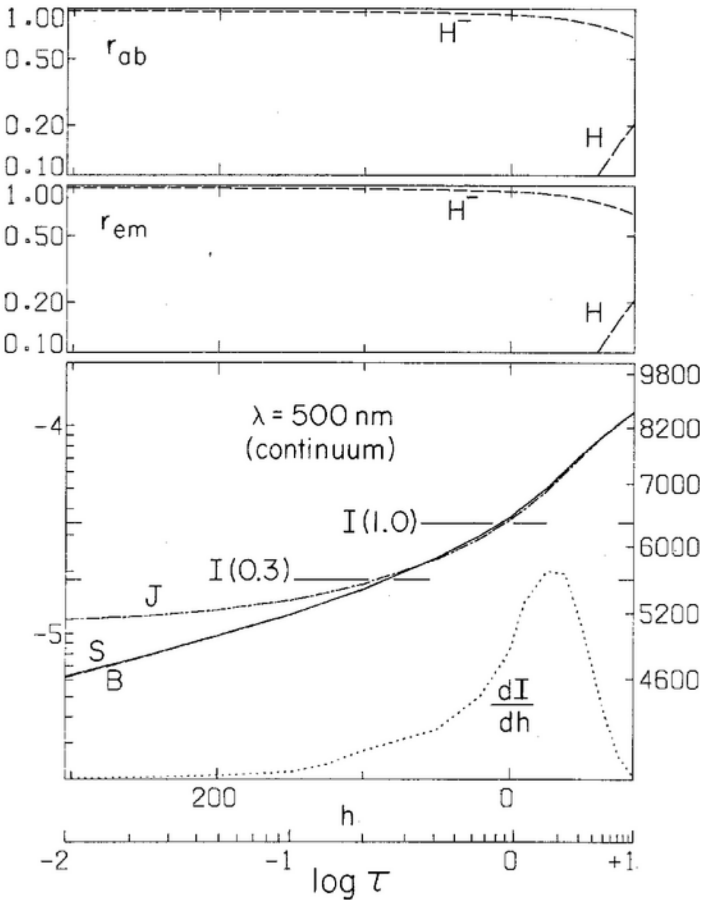

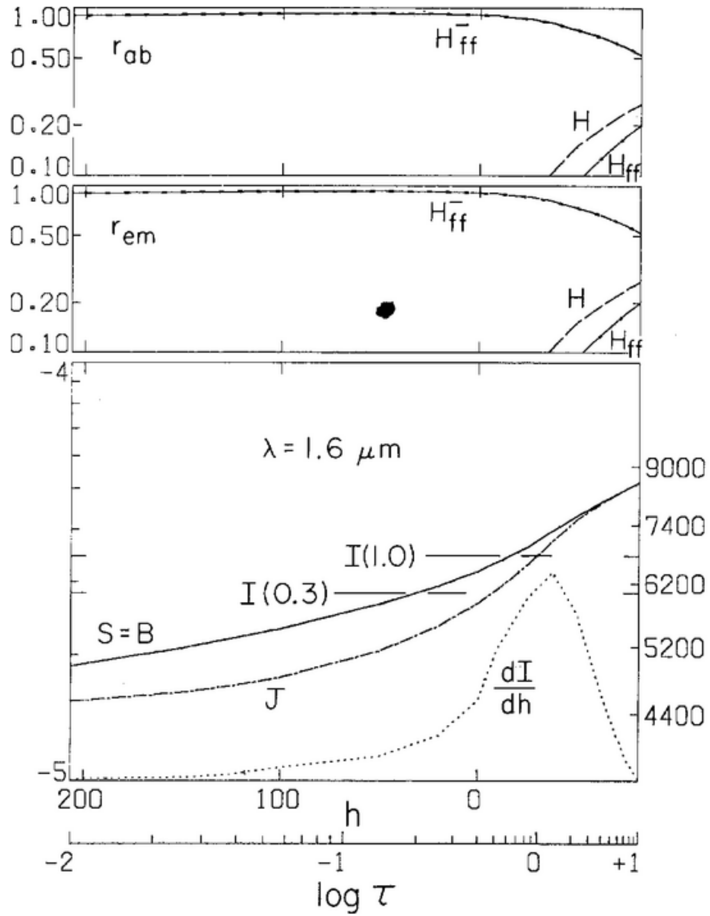

VAL3C CONTINUUM FORMATION

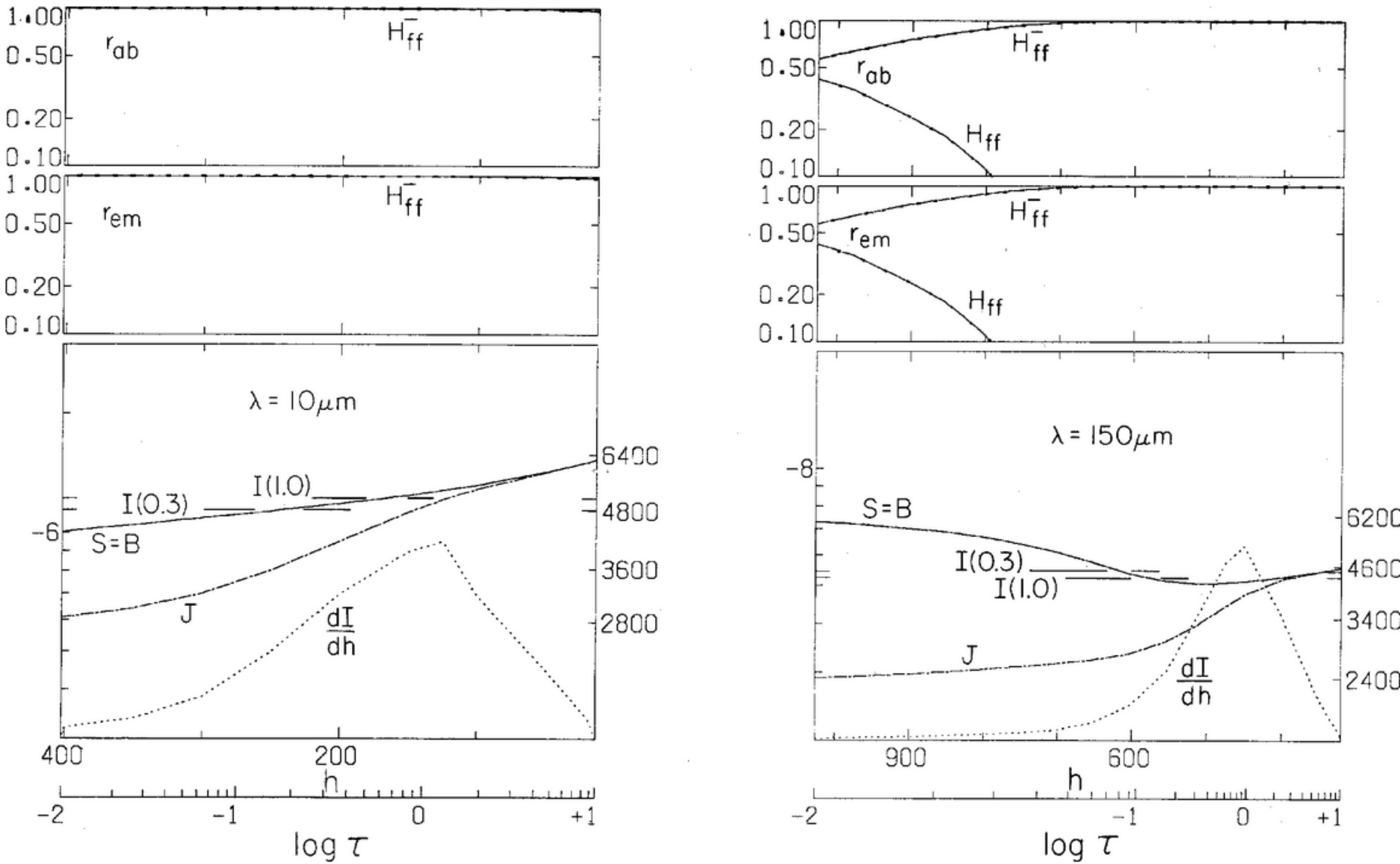

VAL3C CONTINUUM FORMATION

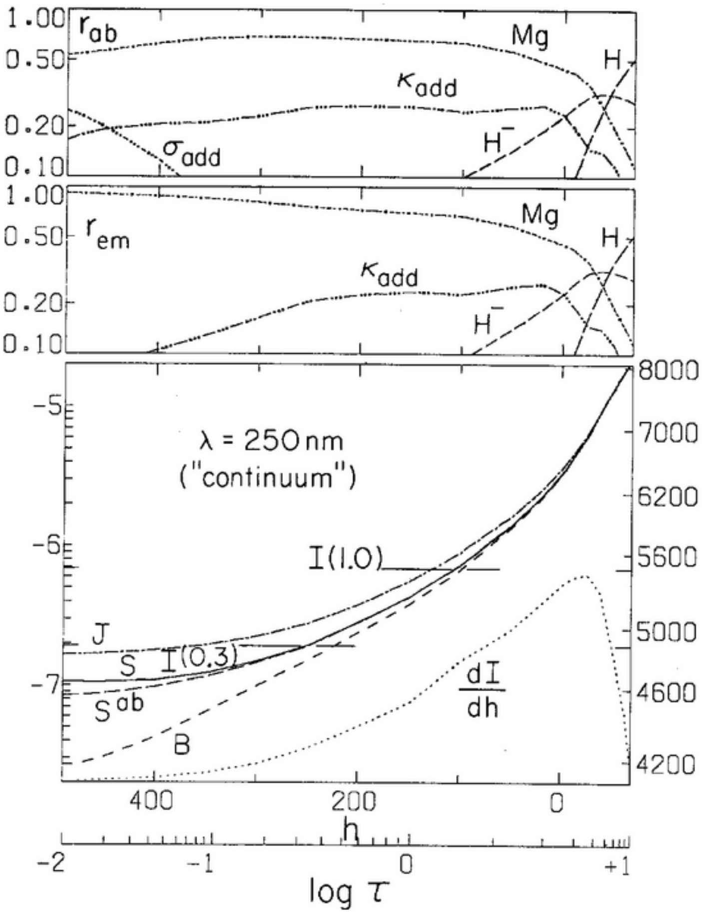

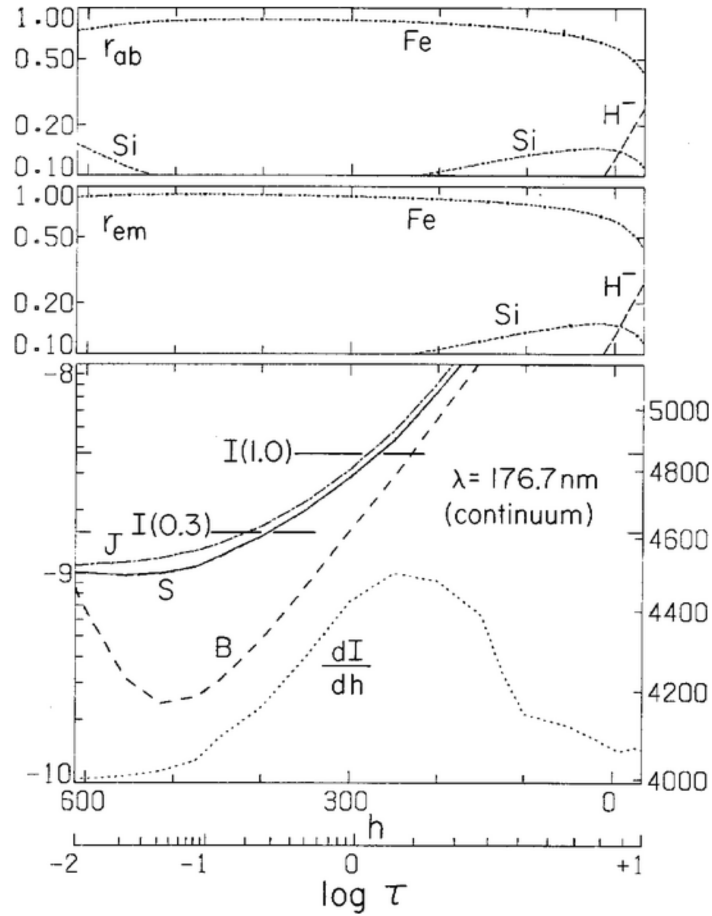

VAL3C CONTINUUM FORMATION

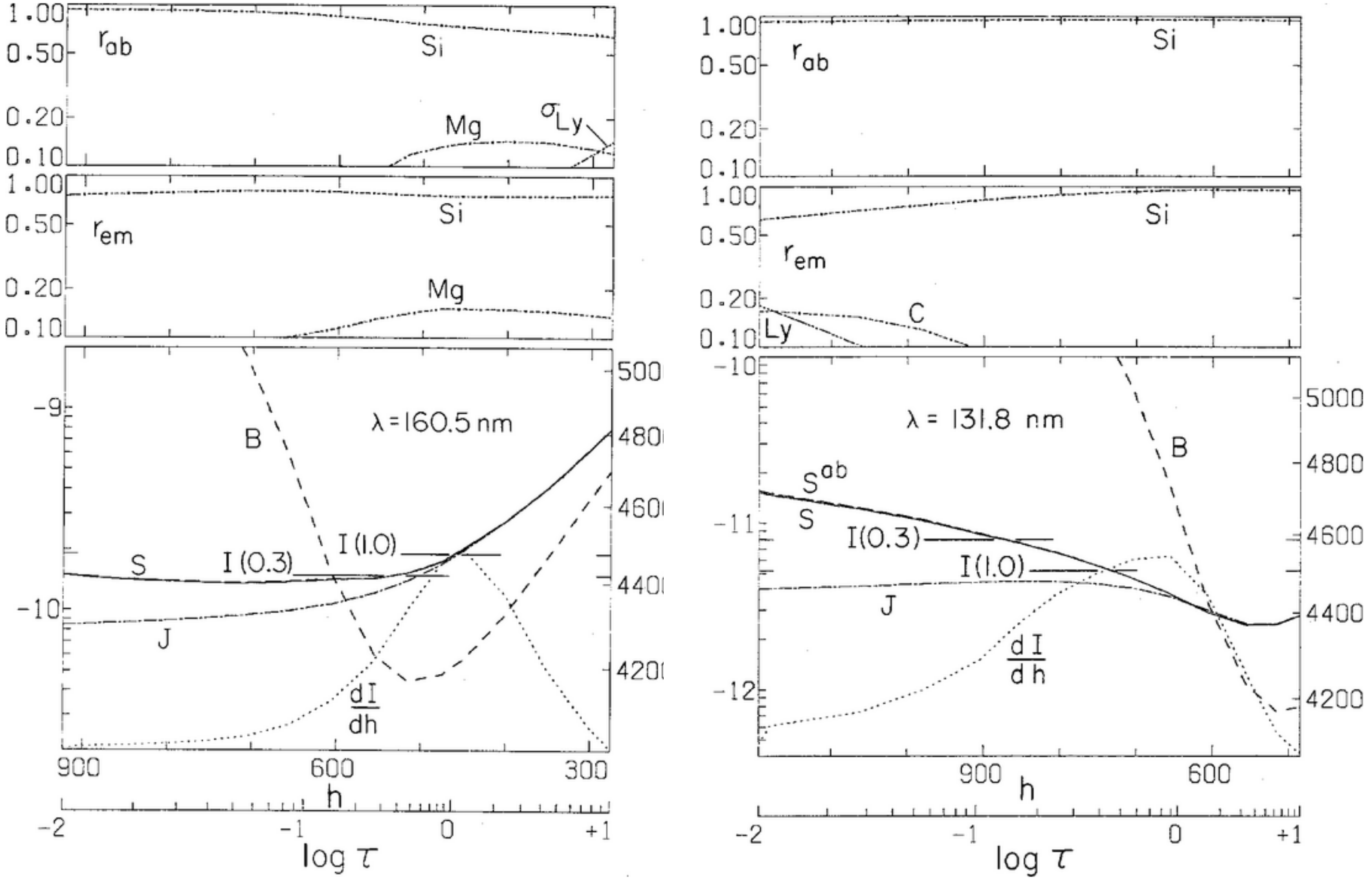

VAL3C CONTINUUM FORMATION

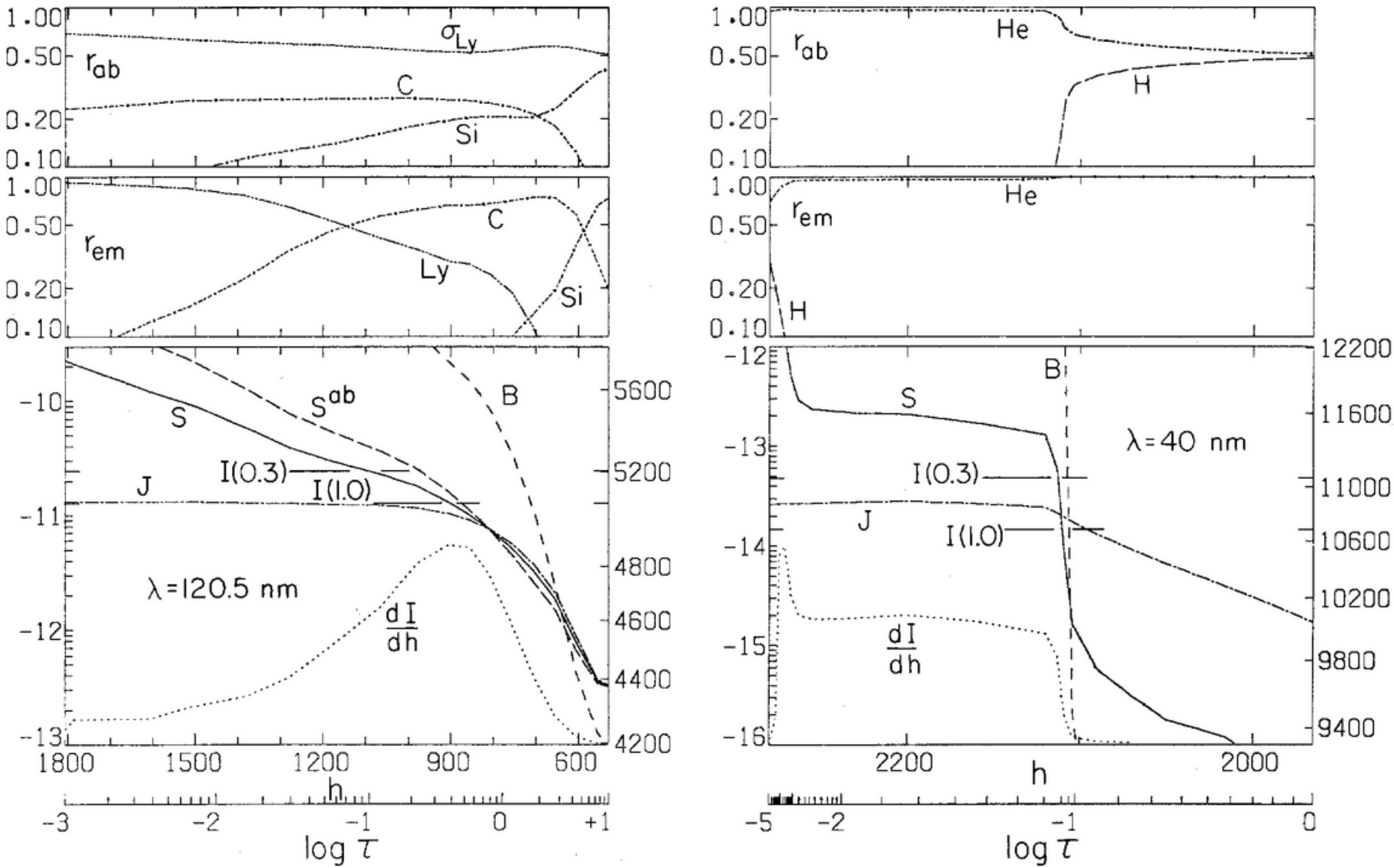

RADIATIVE COOLING

RTSA 7.3.2

Radiative equilibrium condition

$$\begin{aligned}\Phi_{\rm tot}(z) &\equiv \frac{{\rm d}\mathcal{F}_{\rm rad}(z)}{{\rm d}z} = 0 \\ &= 4\pi \int_0^\infty \alpha_\nu(z)\,[S_\nu(z) - J_\nu(z)]\;{\rm d}\nu \\ &= 2\pi \int_0^\infty \int_{-1}^{+1} [j_{\nu\mu}(z) - \alpha_{\nu\mu}(z)\,I_{\nu\mu}(z)]\;{\rm d}\mu\,{\rm d}\nu\end{aligned}$$

Net radiative cooling in a two-level atom gas

$$\begin{aligned}\Phi_{ul} &= 4\pi\alpha^l_{\nu_0}(S^l_{\nu_0} - \overline{J}_{\nu_0}) \\ &= 4\pi j^l_{\nu_0} - 4\pi\alpha^l_{\nu_0}\overline{J}_{\nu_0} \\ &= h\nu_0\left[n_u(A_{ul} + B_{ul}\overline{J}_{\nu_0}) - n_l B_{lu}\overline{J}_{\nu_0}\right] \\ &= h\nu_0\,[n_u R_{ul} - n_l R_{lu}]\end{aligned}$$

Net radiative cooling in a one-level-plus-continuum gas

$$\Phi_{ci} = 4\pi\, n_i^{\rm LTE} b_c \int_{\nu_0}^\infty \sigma_{ic}(\nu)\left[B_\nu\left(1 - \,{\rm e}^{-h\nu/kT}\right) - \frac{b_i}{b_c} J_\nu \left(1 - \frac{b_c}{b_i}\,{\rm e}^{-h\nu/kT}\right)\right]\;{\rm d}\nu$$

VAL3C RADIATION BUDGET

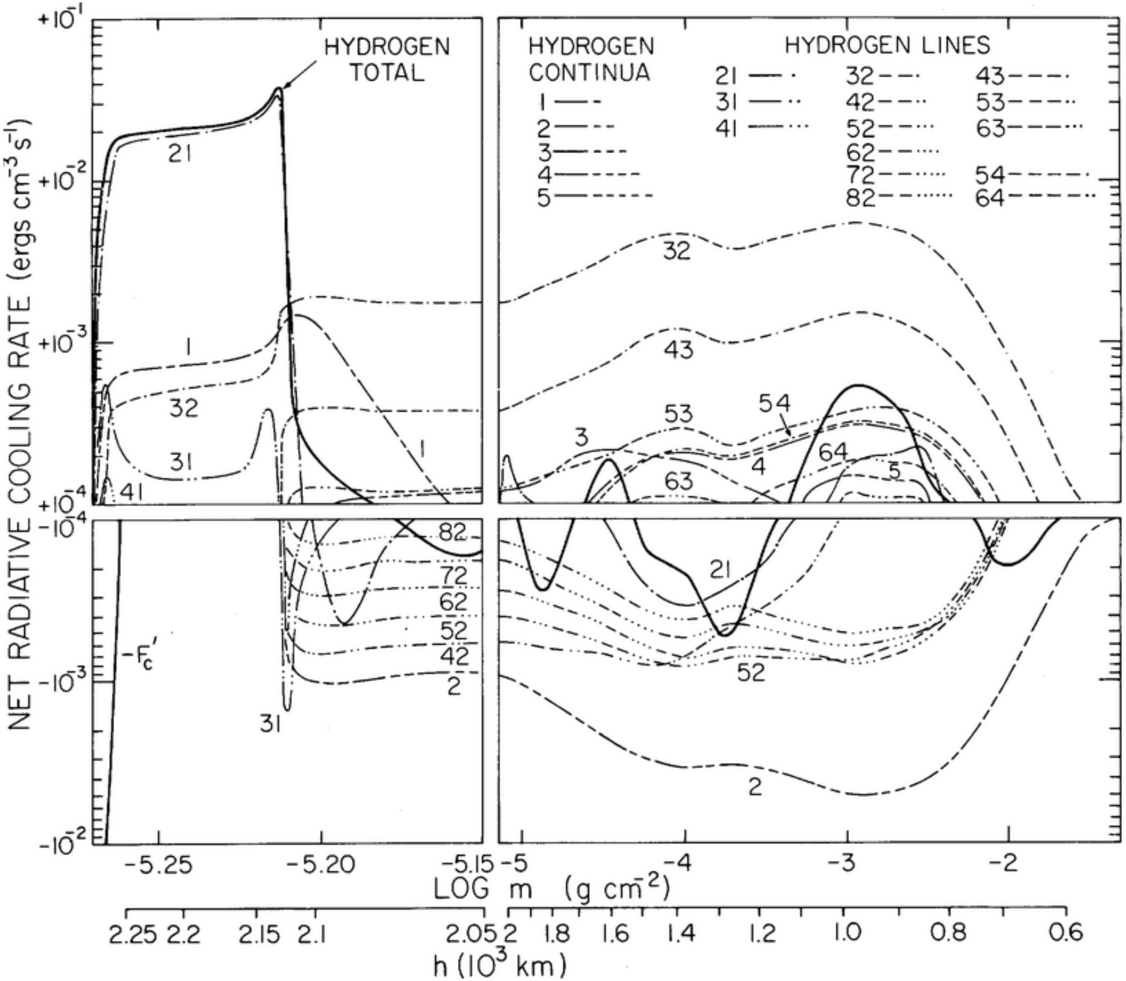

VAL3C RADIATION BUDGET

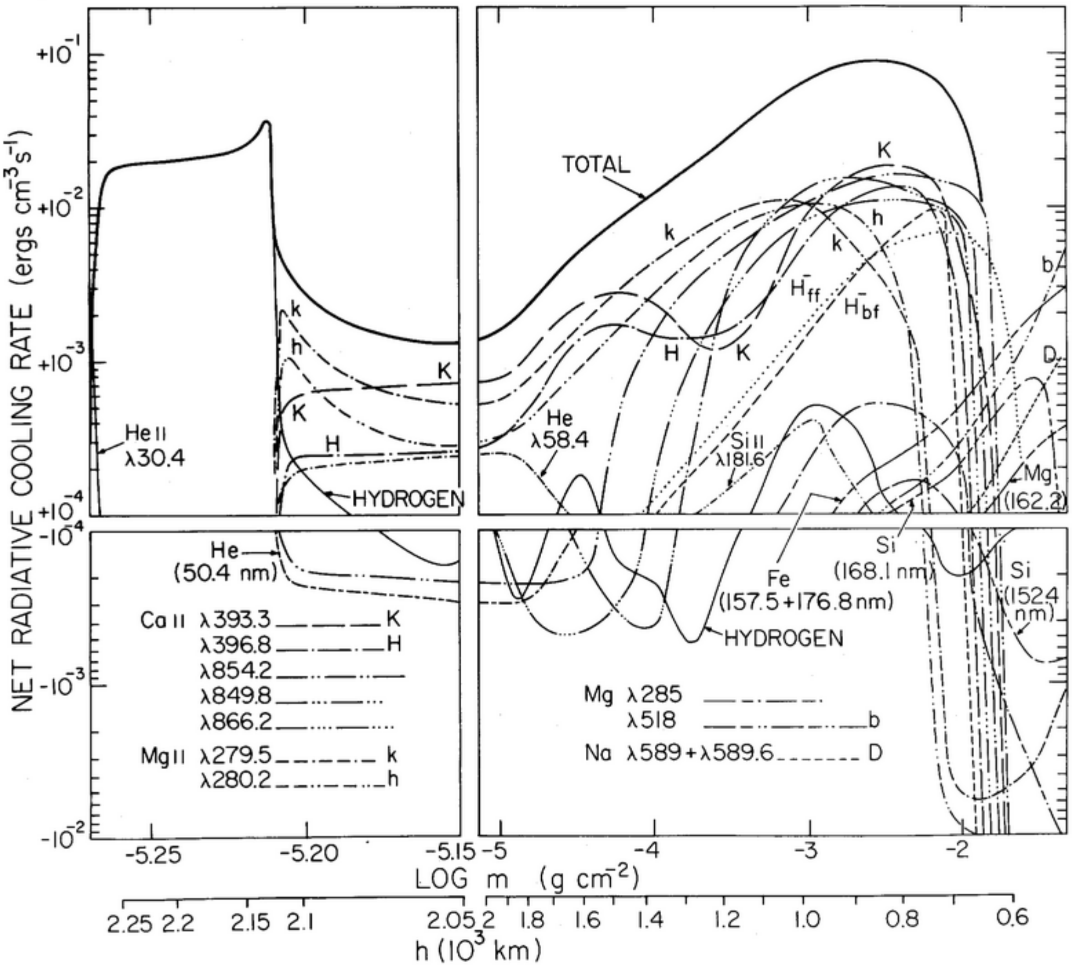

REALISTIC SOLAR ABSORPTION LINE

- extinction: bb peak in $\eta_\nu \equiv \alpha_l/\alpha_c$ becomes lower and narrower at larger height
- optical depth: $\tau_\nu \equiv -\int \alpha_\nu^{\rm total}\,{\rm d}h$ increases nearly log-linearly with geometrical depth
- source function: split for line (bb) and continuous (bf, ff, electron scattering) processes
- intensity: Eddington-Barbier for $S_\nu^{\rm total} = (\alpha_c S_c + \alpha_l S_l)/(\alpha_c + \alpha_l) = (S_C + \eta_\nu S_l)/(1 + \eta_\nu)$

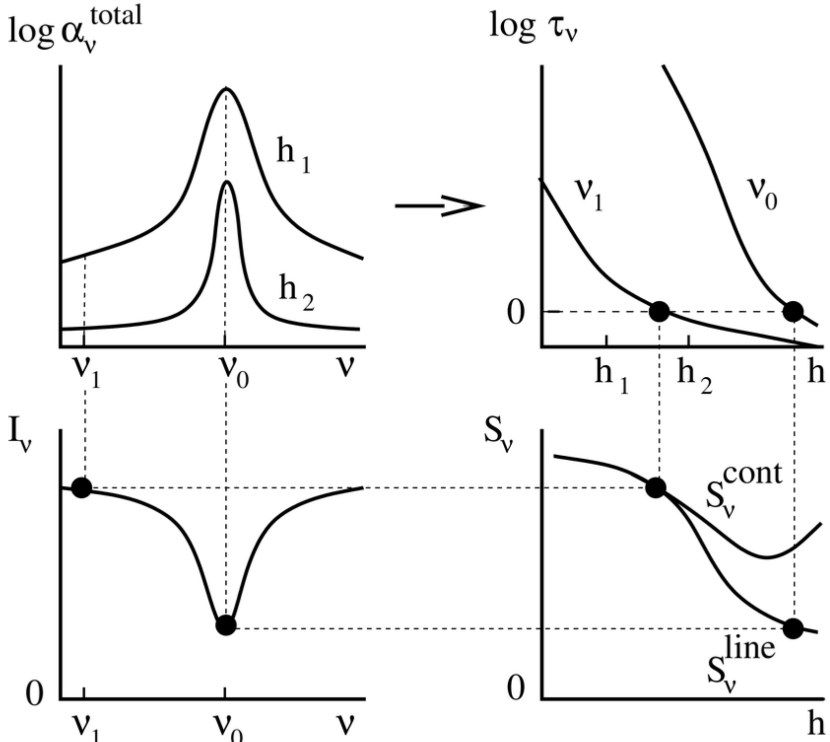

SOLAR NaI D2

NSO disk-center FTS atlas

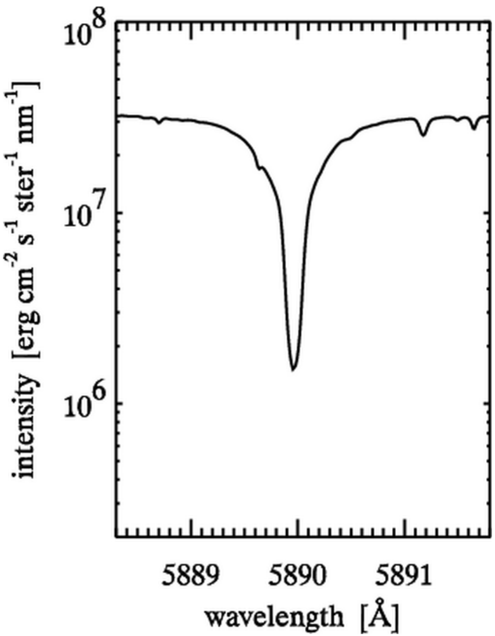

Uitenbroek & Bruls 1992A&A...265..268U

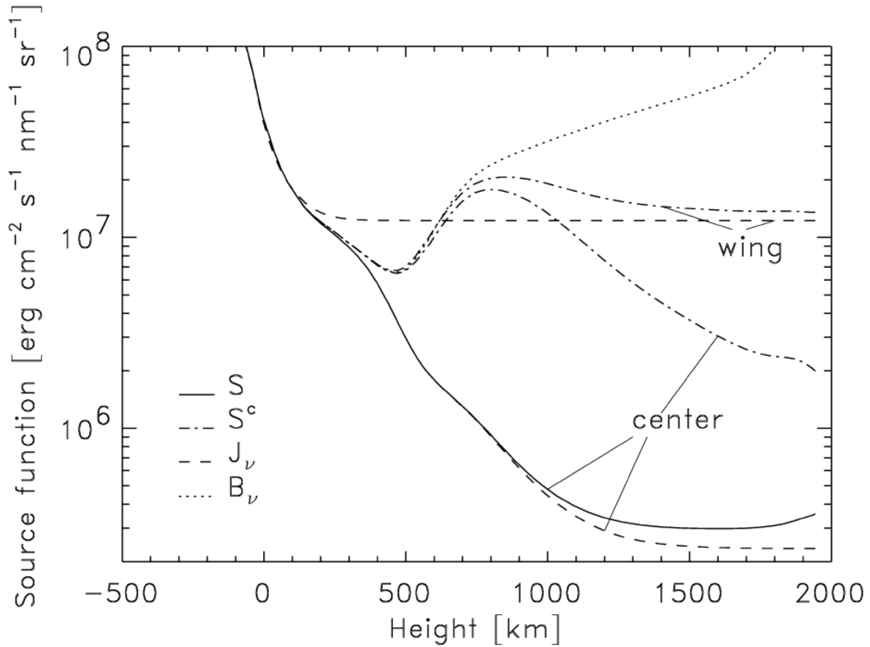

Na I D_2 is a good example of two-level scattering with complete redistribution: very dark

Eddington-Barbier approximation: line-center $\tau = 1$ at $h \approx 600$ km
chromospheric velocity response but photospheric brightness response

What is the formation height of the blend line in the blue wing?

SOLAR NaI D2

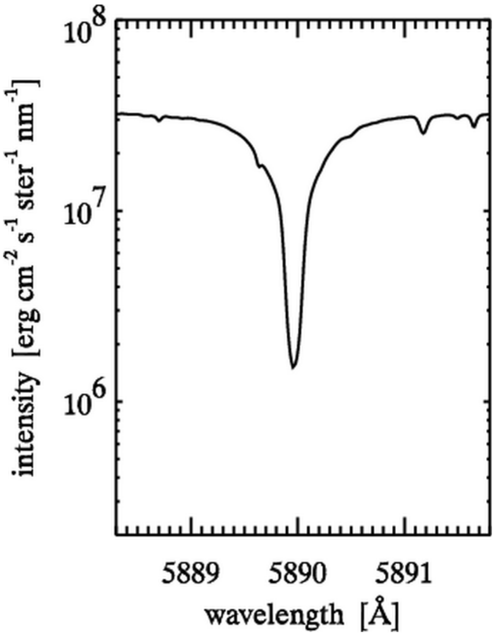

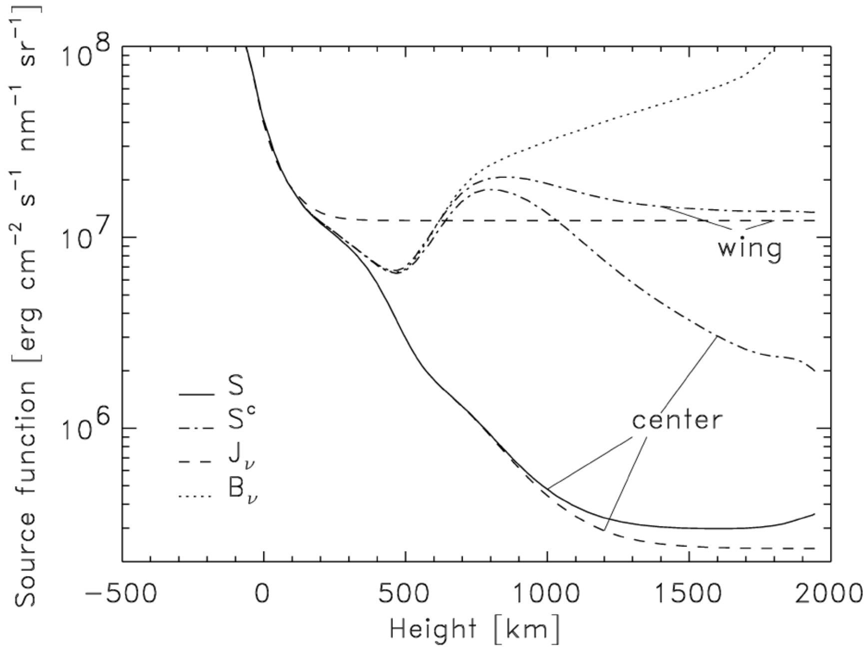

Eddington-Barbier for the blends? Moore, Minnaert, Houtgast 1966sst..book.....M:

5888.703		10.	2.	ATM H2O	R4	302	26
5889.637		14.	2.	ATM H2O	R4	401	26
5889.756	*	752.	4.	ATM H2O	R3	401	26
5889.973M	*	752.	120.SS	NA 1(D2)	0.00	1	
5890.203	*	752.	3.	ATM H2O	R4	302	26
5890.495		5.	1.S"	FE 1P	5.06	1313	
5891.178		17.	3.S	ATM H2O	R3	401	17,26
5891.178		17.	3.S	FE 1P	4.65	1179	

Ca II 8542 VERSUS H-alpha IN 1D NLTE

Cauzzi et al. 2007A&A...503..577C

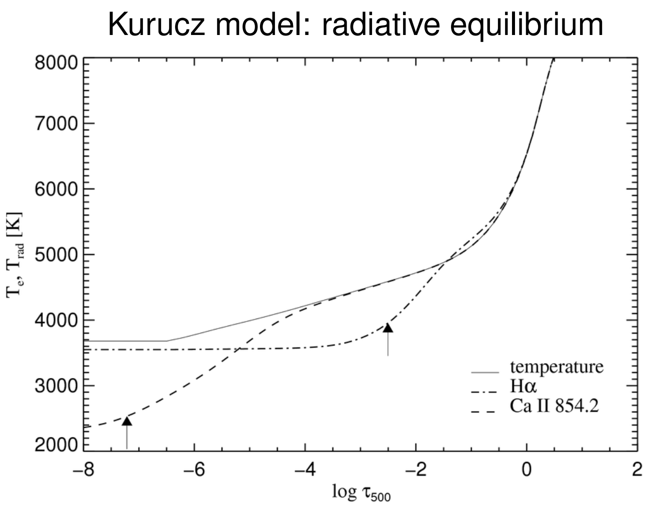

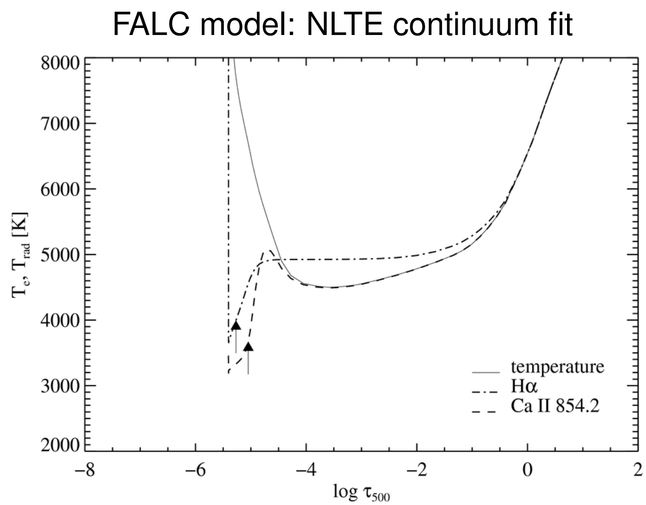

Demonstration of difference in temperature sensitivity between Ca II 854.2 nm and Hα. Each panel shows the temperature stratification of a standard solar model atmosphere and the resulting total source functions S_λ at the nominal line-center wavelengths for Ca II 854.2 nm and Hα, as function of the continuum optical depth at $\lambda = 500$ nm and with the source functions expressed as formal temperatures through Planck function inversion. The arrows mark $\tau = 1$ locations. *Lefthand panel*: radiative-equilibrium model KURUCZ from Kurucz (1979, 1992a, 1992b). It was extended outward assuming constant temperature in order to reach the optically thin regime in Ca II 854.2 nm. *Righthand panel*: empirical continuum-fitting model FALC of Fontenla et al. (1993). Its very steep transition region lies beyond the top of the panel but causes the near-vertical source function increases at left.

SAME WITH RADIATION FIELD

Courtesy Han Uitenbroek

Kurucz model: radiative equilibrium

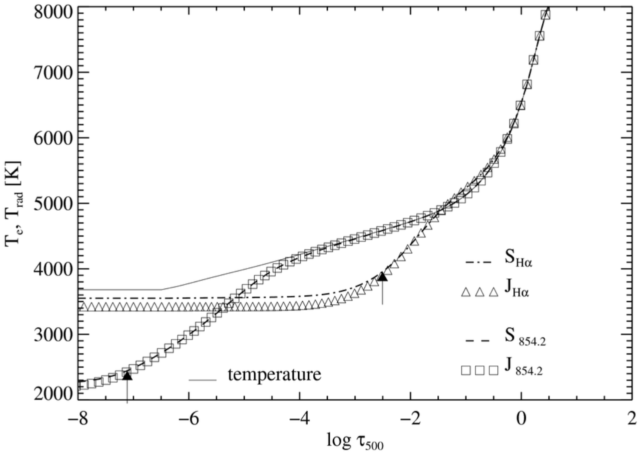

FALC model: NLTE continuum fit

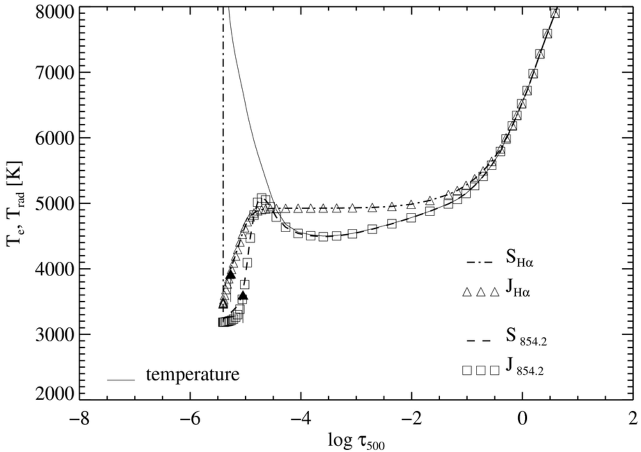

Two-level scattering with $S_{\nu_0} = (1 - \varepsilon_{\nu_0}) J_{\nu_0} + \varepsilon_{\nu_0} B_{\nu_0}$ dominates each source function

SOLAR SPECTRUM FORMATION

Robert J. Rutten

[Sterrekundig Instituut Utrecht & Institutt for Teoretisk Astrofysikk Oslo]

Texts: R.J. Rutten, *"Radiative Transfer in Stellar Atmospheres"* (RTSA), my website
D. Mihalas, *"Stellar Atmospheres"*, 1970, 1978
G.B. Rybicki and A.P. Lightman, *"Radiative Processes in Astrophysics"*, 1979, 2004
M. Stix, *"The Sun"*, 1989, 2002/2004

examples of local, nonlocal, converted photons: white light corona coronium lines EUV corona EUV bright/dark [Zanstra & Bowen PN lines]

radiative transfer basics: basic quantities constant S_ν plane-atmosphere RT Eddington-Barbier cartoons

LTE 1D solar radiation escape: Planck continuous opacity LTE continuum Boltzmann-Saha LTE line equations LTE line cartoons solar ultraviolet spectrum VALIIIC temperature solar spectrum formation Ca II H&K versus Halpha

NLTE 1D solar radiation escape: bb processes bb rates bb equilibria scattering solar radiation processes VAL3C continuum formation radiative cooling VAL3C radiation budget realistic line cartoon Na D1 Ca II 8542 versus Halpha

MHD-simulated essolar radiation escape: Ca II H in 1D Na D1 in 3D non-E hydrogen in 2D

summary: RTSA rap

Ca II H_{2V} GRAIN SIMULATION

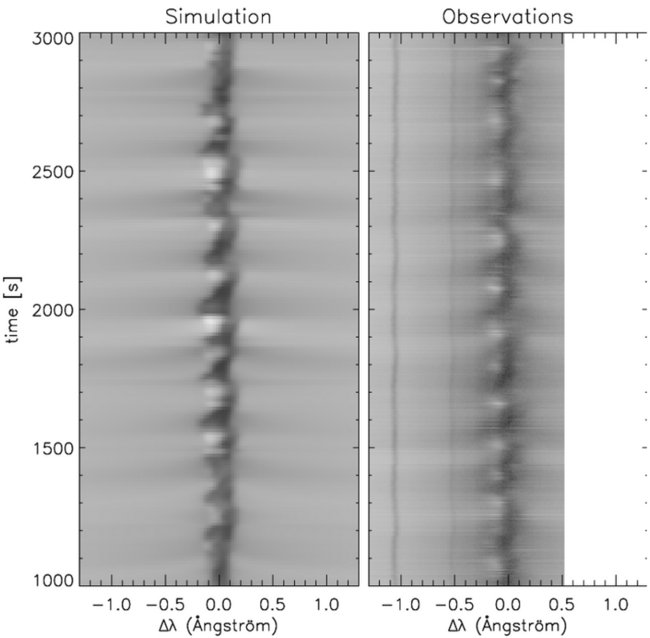

- observation
  Lites, Rutten & Kalkofen 1993
  - sawtooth line-center shift
  - triangular whiskers
  - H_{2V} grains
- simulation
  Carlsson & Stein 1997
  - 1D radiation hydrodynamics
  - subsurface piston from Fe I blend
  - observer's diagnostics
- analysis
  (*RR radiative transfer course*)
  - source function breakdown
  - dynamical chromosphere
  - H_{2V} grains = acoustic shocks

SHOCK GRAIN DIAGNOSIS

Carlsson & Stein, ApJ 481, 500, 1997

$$I_\nu(0) = \int_0^\infty S_\nu \;\; \mathrm{e}^{-\tau_\nu} \;\; \mathrm{d}\tau_\nu = \int_0^\infty S_\nu \;\; \tau_\nu \, \mathrm{e}^{-\tau_\nu} \;\; \frac{\mathrm{d}\ln\tau_\nu}{\mathrm{d}z} \;\; \mathrm{d}z$$

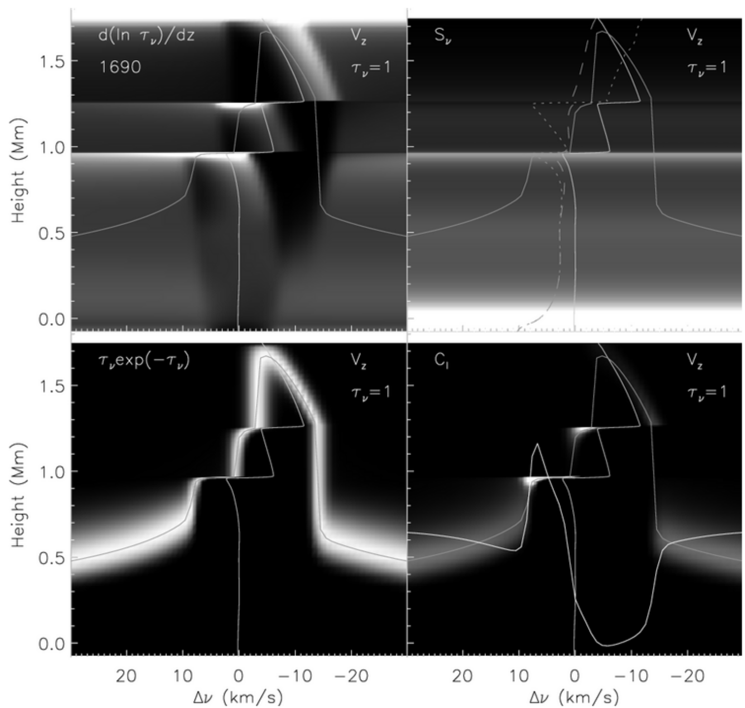

DYNAMIC LOWER CHROMOSPHERE

Carlsson & Stein, ApJ 440, L29, 1995

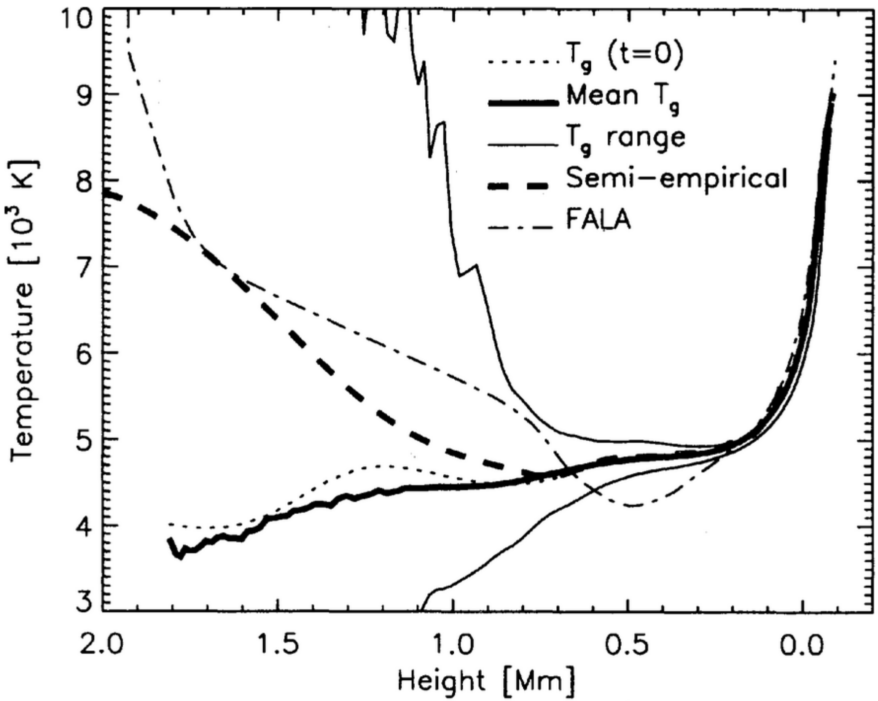

3D NLTE-SE Na D1 IN 3D MHD SIMULATION

Leenaarts et al. 2010ApJ...709.1362L

THE QUIET SOLAR ATMOSPHERE OBSERVED AND SIMULATED IN Na I D_1

J. Leenaarts[1,2,3], R. J. Rutten[1,3], K. Reardon[4,5,6], M. Carlsson[1,2], and V. Hansteen[1,2]
[1] Institute of Theoretical Astrophysics, University of Oslo, P.O. Box 1029, Blindern, N-0315 Oslo, Norway; jorritl@astro.uio.no
[2] Center of Mathematics for Applications, University of Oslo, P.O. Box 1053, Blindern, N-0316 Oslo, Norway
[3] Sterrekundig Instituut, Utrecht University, Postbus 80 000, NL-3508 TA, Utrecht, The Netherlands
[4] INAF-Osservatorio Astrofisico di Arcetri, Largo Enrico Fermi 5, I-50125 Firenze, Italy
[5] Astrophysics Research Centre, Queen's University, Belfast, BT7 1NN, UK
[6] NSO/Sacramento Peak, P.O. Box 62, Sunspot, NM 88349-0062, USA
Received 2009 May 10; accepted 2009 December 15; published 2010 January 13

ABSTRACT

The Na I D_1 line in the solar spectrum is sometimes attributed to the solar chromosphere. We study its formation in quiet-Sun network and internetwork. We first present high-resolution profile-resolved images taken in this line with the imaging spectrometer Interferometric Bidimensional Spectrometer at the Dunn Solar Telescope and compare these to simultaneous chromospheric images taken in Ca II 8542 Å and Hα. We then model Na I D_1 formation by performing three-dimensional (3D) non-local thermodynamic equilibrium profile synthesis for a snapshot from a 3D radiation-magnetohydrodynamics simulation. We find that most Na I D_1 brightness is not chromospheric but samples the magnetic concentrations that make up the quiet-Sun network in the photosphere, well below the height where they merge into chromospheric canopies, with aureoles from 3D resonance scattering. The line core is sensitive to magneto-acoustic shocks in and near magnetic concentrations, where shocks occur deeper than elsewhere, and may provide evidence of heating deep within magnetic concentrations.

SIMULATION PROPERTIES

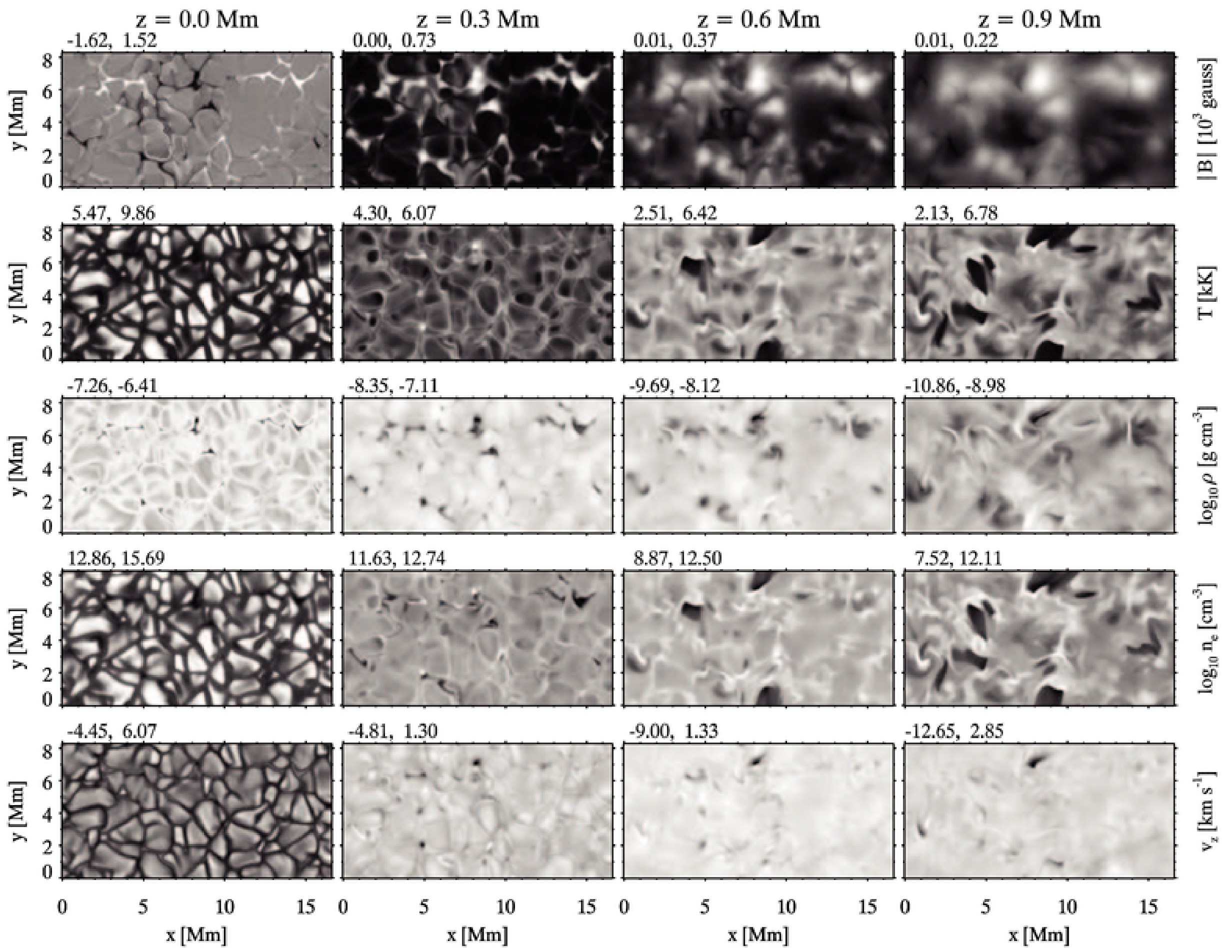

MAGNETIC CONCENTRATION

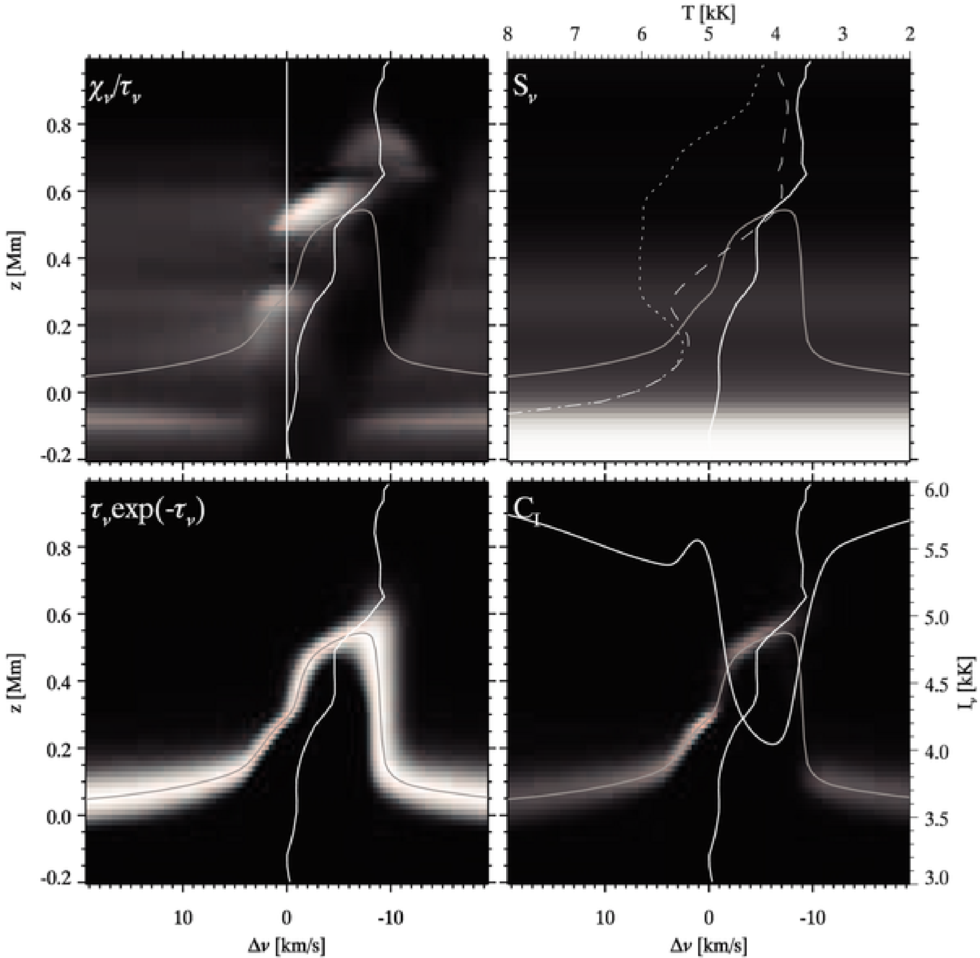

COOL CLOUD

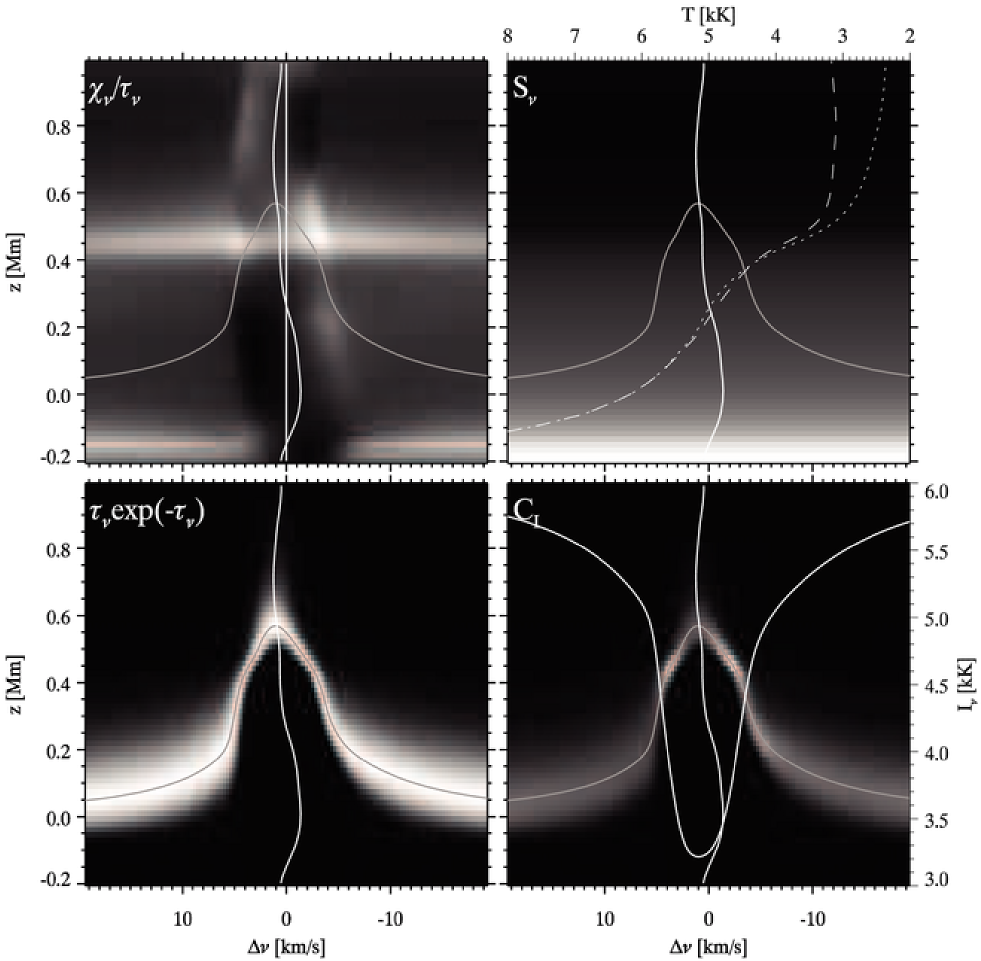

χ_ν/τ_ν
S_ν
$\tau_\nu \exp(-\tau_\nu)$
C_I
T [kK]
8
7
6
5
4
3
2
z [Mm]
0.8
0.6
0.4
0.2
0.0
-0.2
I_ν [kK]
6.0
5.5
5.0
4.5
4.0
3.5
3.0
10
0
-10
Δν [km/s]

HOT FRONT

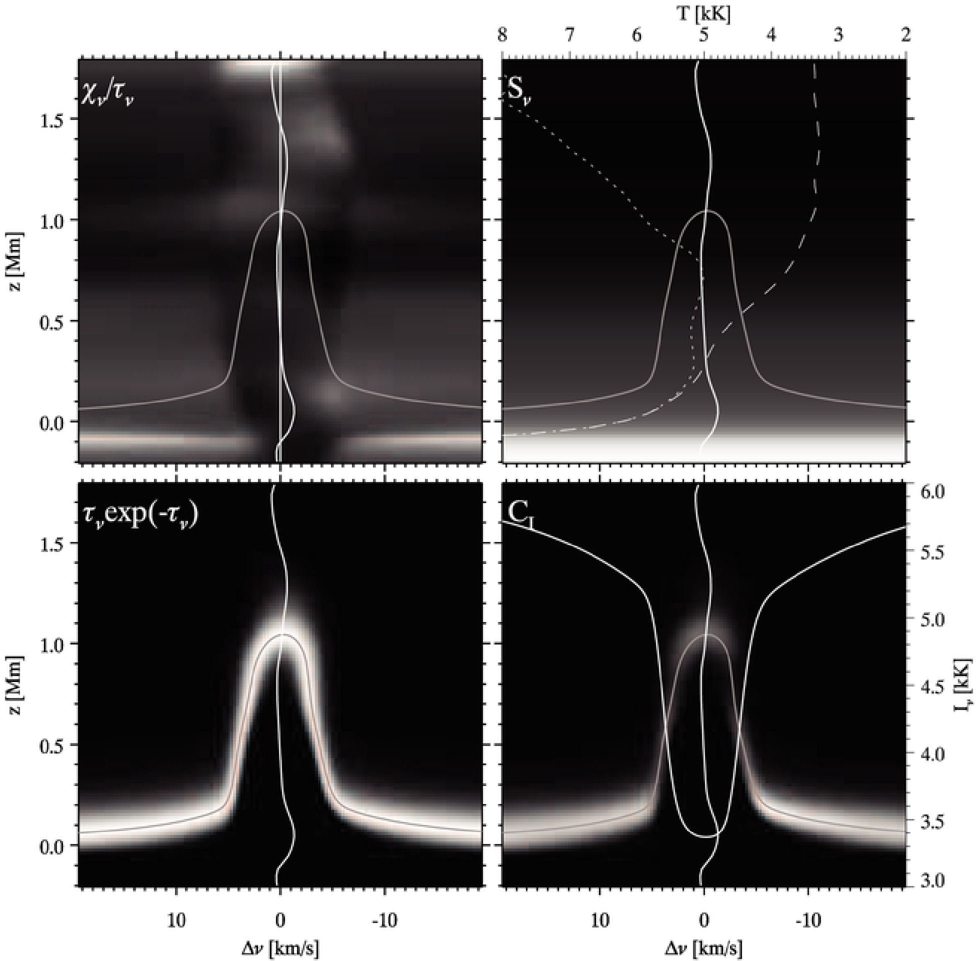

T [kK]
8
7
6
5
4
3
2
χ_ν/τ_ν
S_ν
$\tau_\nu \exp(-\tau_\nu)$
C_I
z [Mm]
1.5
1.0
0.5
0.0
I_ν [kK]
6.0
5.5
5.0
4.5
4.0
3.5
3.0
10
0
-10
$\Delta\nu$ [km/s]

NON-E HYDROGEN IONIZATION

Leenaarts et al. 2007A&A...473..625L

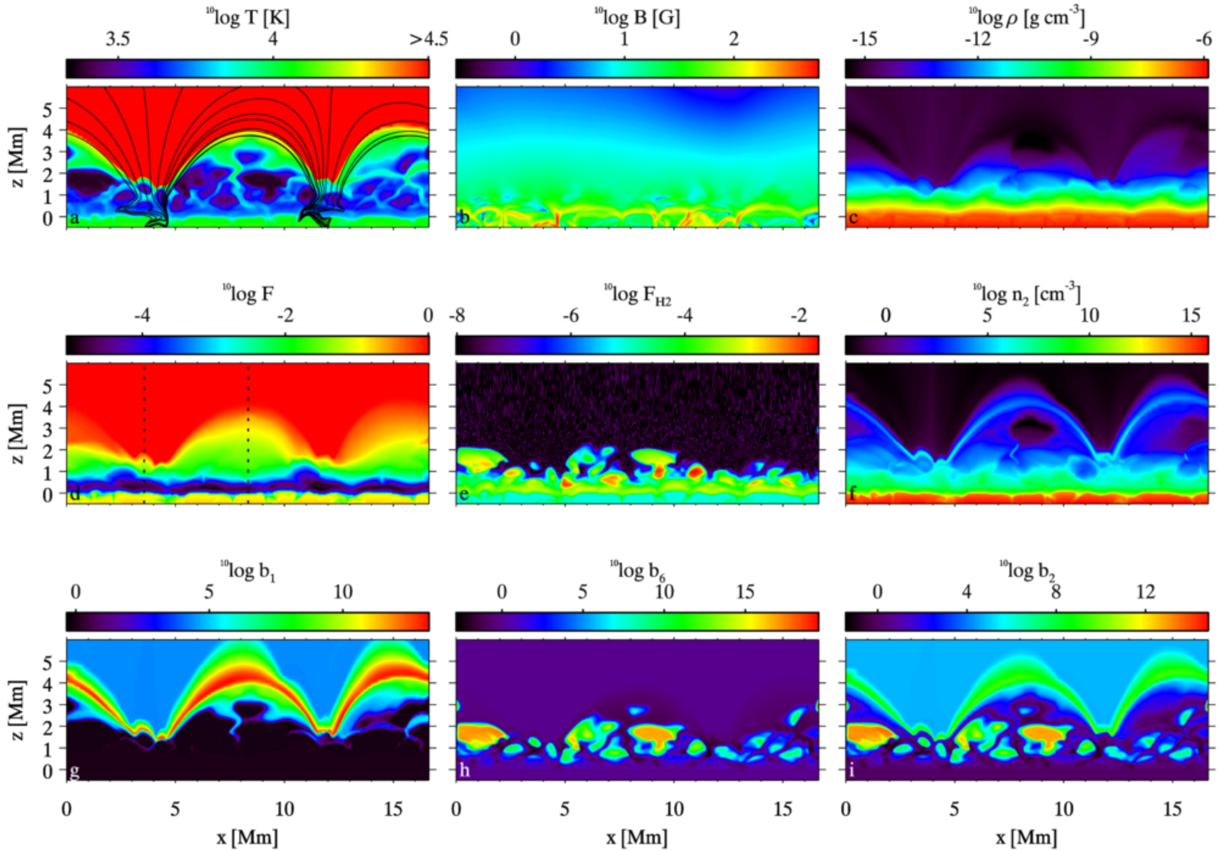

time evolution along the two cuts in the 4th panel

SOLAR SPECTRUM FORMATION

Robert J. Rutten

[Sterrekundig Instituut Utrecht & Institutt for Teoretisk Astrofysikk Oslo]

Texts: R.J. Rutten, *“Radiative Transfer in Stellar Atmospheres”* (RTSA), my website
D. Mihalas, *“Stellar Atmospheres”*, 1970, 1978
G.B. Rybicki and A.P. Lightman, *“Radiative Processes in Astrophysics”*, 1979, 2004
M. Stix, *“The Sun”*, 1989, 2002/2004

examples of local, nonlocal, converted photons: white light corona coronium lines EUV corona EUV bright/dark [Zanstra & Bowen PN lines]

radiative transfer basics: basic quantities constant S_ν plane-atmosphere RT Eddington-Barbier cartoons

LTE 1D solar radiation escape: Planck continuous opacity LTE continuum Boltzmann-Saha LTE line equations LTE line cartoons solar ultraviolet spectrum VALIIIC temperature solar spectrum formation Ca II H&K versus Halpha

NLTE 1D solar radiation escape: bb processes bb rates bb equilibria scattering solar radiation processes VAL3C continuum formation radiative cooling VAL3C radiation budget realistic line cartoon Na D1 Ca II 8542 versus Halpha

MHD-simulated essolar radiation escape: Ca II H in 1D Na D1 in 3D non-E hydrogen in 2D

summary: RTSA rap

BASIC RADIATIVE TRANSFER EQUATIONS

RTSA last page

specific intensity	$I_\nu(\vec{r}, \vec{l}, t)$ erg cm^{-2} s^{-1} Hz^{-1} ster^{-1}
emissivity	j_ν erg cm^{-3} s^{-1} Hz^{-1} ster^{-1}
extinction coefficient	α_ν cm^{-1} σ_ν cm^2 part^{-1} κ_ν cm^2 g^{-1}
source function	$S_\nu = \sum j_\nu / \sum \alpha_\nu$
radial optical depth	$\tau_\nu(z_0) = \int_{z_0}^{\infty} \alpha_\nu \, \mathrm{d}z$
plane-parallel transport	$\mu \, \mathrm{d}I_\nu / \mathrm{d}\tau_\nu = I_\nu - S_\nu$
thin cloud	$I_\nu = I_0 + (S_\nu - I_0) \, \tau_\nu$
thick emergent intensity	$I_\nu^+(0, \mu) = \int_0^\infty S_\nu(\tau_\nu) \, \mathrm{e}^{-\tau_\nu/\mu} \, \mathrm{d}\tau_\nu / \mu$
Eddington-Barbier	$I_\nu^+(0, \mu) \approx S_\nu(\tau_\nu = \mu)$
mean mean intensity	$\overline{J}_{\nu_0}^{\varphi} = \frac{1}{2} \int_0^\infty \int_{-1}^{+1} I_\nu \, \varphi(\nu - \nu_0) \, \mathrm{d}\mu \, \mathrm{d}\nu$
photon destruction	$\varepsilon_\nu = \alpha_\nu^{\mathrm{a}} / (\alpha_\nu^{\mathrm{a}} + \alpha_\nu^{\mathrm{s}}) \approx C_{ul} / (A_{ul} + C_{ul})$
complete redistribution	$S_{\nu_0}^l = (1 - \varepsilon_{\nu_0}) \, \overline{J}_{\nu_0}^{\varphi} + \varepsilon_{\nu_0} B_{\nu_0}$
isothermal atmosphere	$S_{\nu_0}(0) = \sqrt{\varepsilon_{\nu_0}} \, B_{\nu_0}$